Article

Lymphopenia-induced lymphoproliferation drives activation of naive T cells and expansion of regulatory populations

Lymphopenia induced proliferation post-transplant

Eldershaw S,
Verma K, Croft
W, ..., Zuo J,
Malladi R, Moss P

p.moss@bham.ac.uk

HIGHLIGHTS
Lymphopenia drives
global T cell activation
with selective FoxP3+
T cell proliferation

naive T cells undergo TCR-
mediated activation and
effector populations
expand

IL-7R is downregulated on
all T cell subsets whilst IL-
2Rα expression increases

Fatty acid metabolism &
interferon-signaling
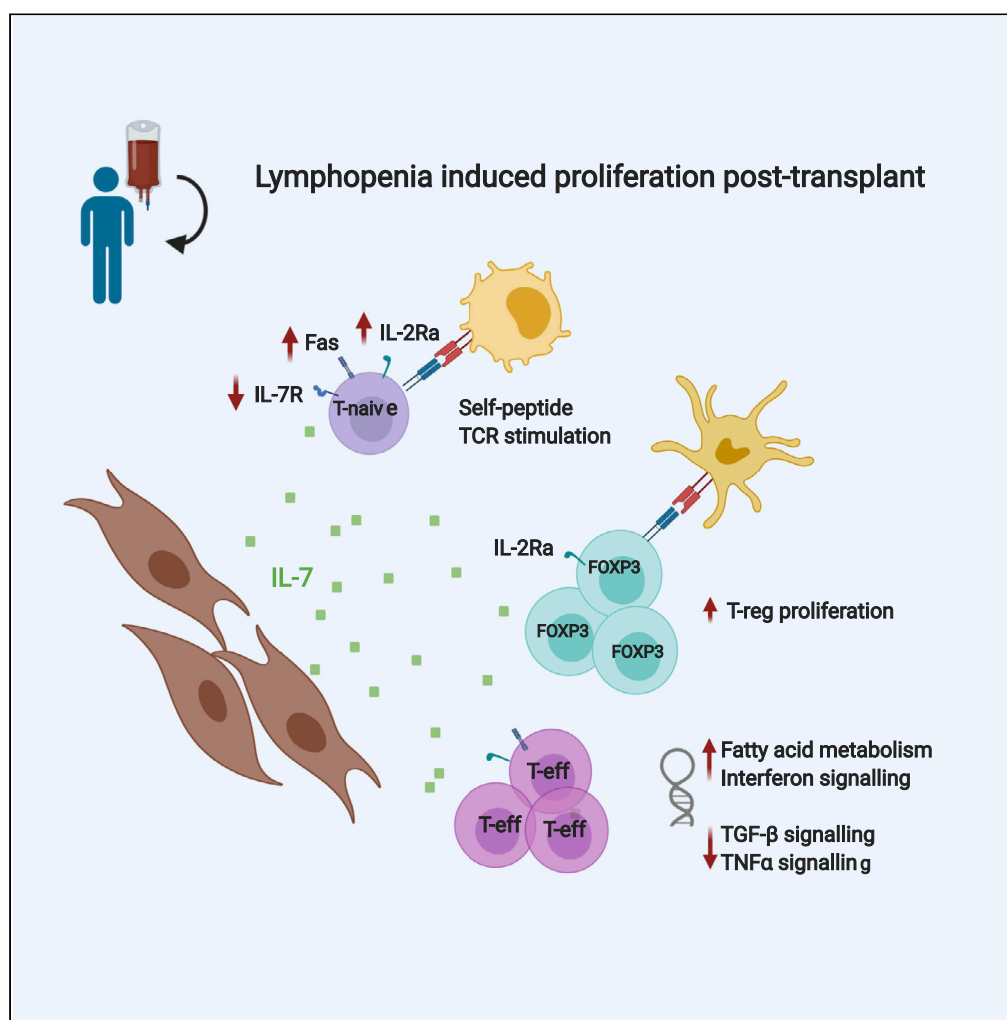increase; TGF-β responses
suppressed

Article

Lymphopenia-induced lymphoproliferation drives activation of naive T cells and expansion of regulatory populations

Eldershaw S,[1,4] Verma K,[1,4] Croft W,[1,2,4] Rai T,[1] Kinsella FAM,[1,3] Stephens C,[1] Chen H,[1] Nunnick J,[3] Zuo J,[1] Malladi R,[3] and Moss P[1,2,5,*]

SUMMARY

Chemotherapy pre-conditioning is an essential component of chimeric antigen receptor transduced cell therapy. Acute lymphopenia-induced proliferation (LIP) is known to be driven primarily by homeostatic cytokines, but little is known on the underlying mechanisms in humans. We undertook phenotypic and transcriptional analysis of T cells undergoing LIP two weeks post-myeloablative autograft stem cell transplantation. Strong IL-7 signaling was reflected in downregulated IL-7R expression on all T cells, including naive cells, along with parallel increased IL-2Rα expression. Notably, activated residual naive cells expressed Fas indicating recent TCR engagement. Moreover, proportion of Ki67 + FoxP3+ Tregs was almost doubled. Transcriptional analysis revealed increased fatty acid metabolism and interferon signaling responses. In contrast, TGF-β signaling was strongly suppressed. Thus, human LIP response is characterized by cytokine and TCR-driven proliferation which drives global T cell activation but also preferentially triggers regulatory cell expansion which may limit tumor-specific immunity. These features indicate potential therapeutic opportunities to manipulate immunotherapy regimens incorporating LIP conditioning protocols.

INTRODUCTION

A characteristic feature of the immune system is the maintenance of a stable lymphoid pool with relatively little fluctuation in lymphocyte number over time. Homeostatic proliferation is one mechanism by which this is achieved and refers to the ability of lymphoid cells to increase proliferation during periods of acute and chronic lymphopenia (Takada and Jameson, 2009) (Mackall and Gress, 1997).

The homeostatic cytokines IL-7 and IL-15 are important mediators in this regard with IL-7 acting as a primary 'rheostat' through its proliferative and anti-apoptotic activity. IL-7 is produced by a range of stromal cells and serum concentrations are regulated through consumption by lymphoid populations (Martin et al., 2017). IL-7 concentrations therefore increase during lymphopenia (Condomines et al., 2010) and act to drive increased lymphoproliferation (Perales et al., 2012). In contrast, IL-15 mediates its effect primarily on memory CD8+ T cells and natural killer cells. Profound lymphopenia leads to lymphopenia-induced proliferation (LIP) and in this setting murine models indicate that T cell receptor engagement also promotes proliferation through recognition of self-peptides by naive T cells (Winstead et al., 2010) (Goldrath et al., 2000) (Cho et al., 2016).

Chemotherapy and conditioning regimens used prior to stem cell transplantation lead to profound lymphopenia and mediate a state of acute LIP characterized by intense T cell proliferation. However, the underlying mechanisms that drive this remain uncertain. T cell adoptive therapy, using approaches such as chimeric antigen receptor transduced (CAR-T) cells (Restifo et al., 2012) (Brentjens et al., 2013) (Gattinoni et al., 2005), has transformed the outlook for many patients with malignant disease but the success of this approach is reliant on generation of administration of chemotherapy in order to promote LIP.

Here we undertook a detailed assessment of the phenotypic and transcriptional profile of T-cells following hemopoietic autografting as a model to improve understanding of mechanisms that underlie acute LIP in the human setting. Our hypothesis was that this would be mediated by enhanced TCR and cytokine

[1]Institute of Immunology and Immunotherapy, University of Birmingham, Birmingham, UK

[2]Centre for Computational Biology, University of Birmingham, Birmingham, UK

[3]Center for clinical Haematology, Queen Elizabeth Hospital, Birmingham, UK

[4]These authors contributed equally

[5]Lead contact

*Correspondence: p.moss@bham.ac.uk

https://doi.org/10.1016/j.isci.2021.102164

signaling although details of these remain uncertain and we anticipated that this data set would reveal novel biochemical and transcriptional mechanisms that underlie the proliferative response of T cells in this setting. The translational ambition was that this could be of value in the development of novel CAR-T regimens that facilitate LIP without the use of toxic conditioning regimens. We report that T cells display intense global proliferation, including naive cell activation, mediated by an interferon-driven proliferation fueled by fatty acid metabolism. Unexpectedly, this is associated with enhanced transcription of genes associated with regulatory function and an increase in the proportion of FoxP3+ T regulatory cells. These findings provide new insights into the mechanism of LIP in the human immune system and potentially offer a range of novel translational opportunities.

RESULTS

T cells numbers are very low in first two weeks after autograft transplantation but cells are undergoing intense proliferation

Initial studies were undertaken to determine the T cell count in patients during the early period after hemopoietic autograft transplantation. Blood samples of individual patients were analyzed longitudinally, taken immediately prior to stem cell infusion (day 0) and then on day 7 and day 12 after transplant (n = 41, 58, and 56, respectively). The number of TCRαβ cells was determined using absolute lymphocyte count and flow cytometric analysis.

T cell counts were low on day 0 (0.016×10^9/l) compared to age-matched healthy donors (1.5×10^9/l) and fell further during the first week to undetectable levels. Numbers then significantly increased over the next few days to reach a median value of 0.026×10^9/l on day 12 (Figure 1A). Ki-67 staining was used to measure the proportion of T cells that were undergoing active division. This was measured at 46% of total T cells at day 12 compared to only 1.5% in healthy donors (Figure 1B). T cells are therefore undergoing a very high degree of LIP within the early post-transplant period.

We next determined the relative proportion of CD4+ and CD8+ T cells which represented 60% and 38% of T cells, respectively, on day 0. The proportion of CD4+ cells significantly increased to 75% by day 7 before falling back to 62% on day 12 (Figure 1C). A reciprocal pattern was observed for CD8+ populations (Figure 1D), suggesting that CD4+ T cells have a brief selective proliferative advantage in the first week post-transplant. Nevertheless, no overall difference in the CD4:CD8 ratio was observed in the first two weeks post-transplant.

ELISA was used to determine the serum concentration of IL-7, IL-15, TGF-β1, and IFN-γ during the first 12 days post-transplant (Figure 1E). IL-7 fell from 8.6pg/ml at the time of transplant to a median of 2.6pg/ml at day 12, compatible with peripheral consumption during LIP. In contrast IL-15 concentration at day 0 was 2.5pg/ml, above median values in HD (1.6pg/ml), and increased further to 8.8pg/ml at day 12. TGF-β1 serum levels fell markedly over the first 12 days post-transplant (301.3pg/ml to 45.1pg/ml) but no changes were observed in IFN-γ concentration.

The proportion of naive T cells falls dramatically after transplant whilst effector cells are substantially increased

The expression of CD45RA and CCR7 was then used to delineate the proportion of naive (CD45RA + CCR7+), central memory (CD45RA-CCR7+), effector (CD45RA-CCR7-) and effector memory (CD45RA + CCR7-) cells. The most striking observation was that the proportion of naive cells fell substantially within the first two weeks post-transplant. In particular, these represented 37% of CD4+ cells on day 0 but only 8.6% at day 12 (Figure 2A). The comparable values for CD8+ subsets were 37% and 6.9%, respectively (Figure 2B). This reduction was mirrored by a substantial increase in the proportion of effector cells (EMs) during this period, rising from 11% to 39%, and 18%–53%, within the CD4+ and CD8+ populations, respectively. No significant differences were seen in the relative proportion of central memory or EMRA cells during this period. In order to determine the direct relationship between the proportion of naive and effector memory, we also assessed the relative change within individual patients and a strong correlation was observed (Figure 2C).

Fas expression on naive T cells reveals recent TCR engagement during LIP

Our previous findings, showing a marked reduction in the proportion of naive T cells, led us to investigate if cells with a naive phenotype had undergone TCR-mediated stimulation and differentiation during LIP. As
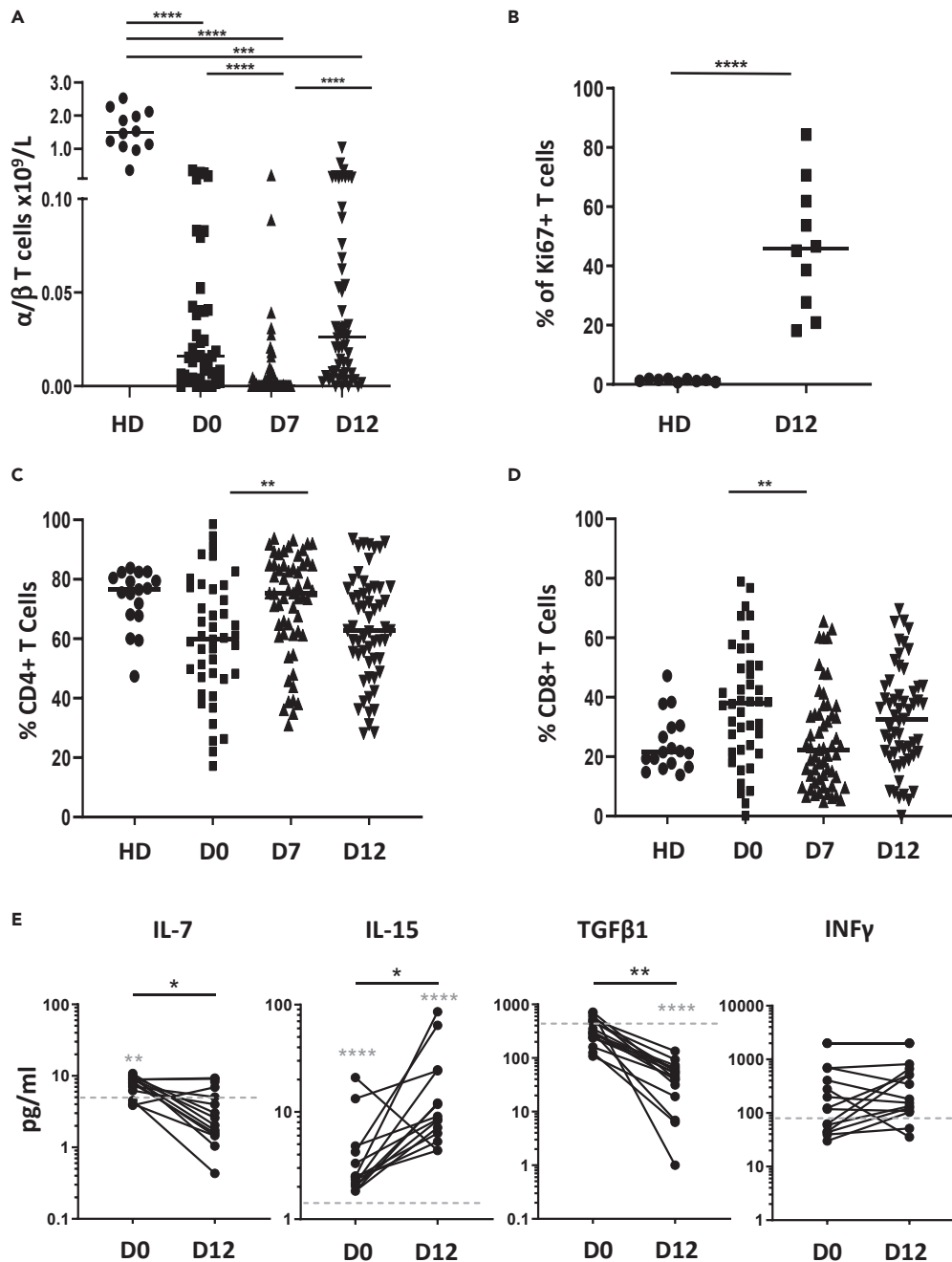
Figure 1. αβ T cell numbers are very low but undergoing intense proliferation in the early lymphopenic environment post-transplant

(A) Absolute count of TCRab T cells at day 0 (D0, n = 41), at day 7 (D7, n = 58) and day 12 (D12, n = 56) post-transplant. Values from healthy donors are also shown (HD, n = 12).

(B) Ki67 staining on T cells from HD (n = 9) and D12 patients (n = 10).

(C and D) (C) Percentage of CD4+ and (D) CD8+ T cells within each group (HD, n = 17; D0, n = 42; D7, n = 57; D12, n = 57).

(E) Serum concentration of cytokines IL-7, IL-15, TGFβ and IFNγ measured in matched D0 and D12 patient samples (n = 14). Gray line depicts the median value in healthy controls. Kruskal-Wallis test with Dunn's multiple comparison test (A,C and D), Wilcoxon signed-rank test (E) and Mann-Whitney U test (B, E(gray)) was performed for statistical analysis, **p < 0.01, ***p < 0.001 and ****p < 0.0001.
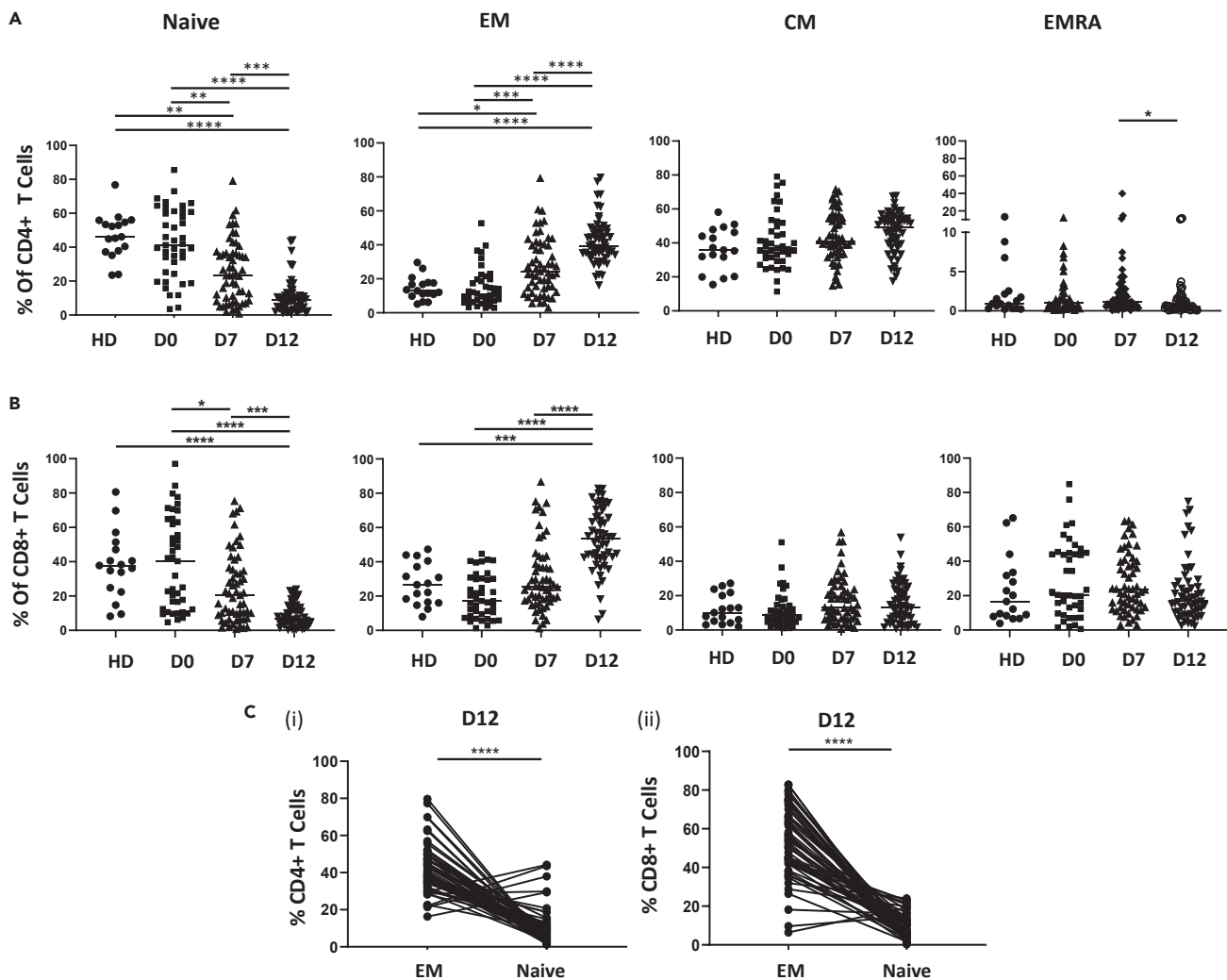
Figure 2. The proportion of naive T cells falls markedly after transplant whilst effector subsets increase

(A and B)Percentage of T cell subsets in (A) CD4+ and (B) CD8+ population in healthy donors (HD, n = 17) and autograft patients at day 0 (D0 n = 41), at Day 7(D7, n = 57) and Day 12 (D12, n = 56) post-transplant.

(C) Paired comparison of proportions of CD4+ (i) and CD8+ (ii) naive and effector memory (EM) subsets in each patient at day 12 post-transplant (n = 56). Bar indicates median value. Kruskal-Wallis test with Dunn's multiple comparison test (A,B) and Wilcoxon matched-pairs signed-ranks test (C) was performed for statistical analysis, *p < 0.05, **p < 0.01, ***p < 0.001, ****p < 0.0001.

such, we examined the expression profile of Fas (CD95) in relation to memory profile. Fifty percent and 64% of global CD4+ and CD8+ T cells expressed Fas at the time of transplant but this increased substantially to reach respective levels of 94% and 96% at D12 (Figure 3A). Assessment of Fas expression in relation to differentiation status revealed a 9.3-fold and 3.5-fold increase of Fas expression on naive CD4+ and CD8+ T cells, respectively. Indeed, Fas expression was seen on over 43% and 69% of phenotypically 'naive' CD4+ and CD8+ T cells, respectively, in the early post-transplant period (Figure 3B). In contrast, no increase in Fas expression was seen on effector or memory subsets in keeping with the stable expression of this marker on antigen-experienced cells (Figure 3C).

T cells undergoing LIP display a reciprocal pattern of IL-7R and IL-2Rα expression

Given the importance of common gamma chain cytokines in homeostatic proliferation we next measured the profile of IL-7R (CD127) and IL-2Rα (CD25) expression on T cell subsets during LIP (Figure S1). IL-7R is downregulated following engagement with its ligand (Francois et al., 2018) and therefore a reduction in expression is representative of recent cytokine activation.
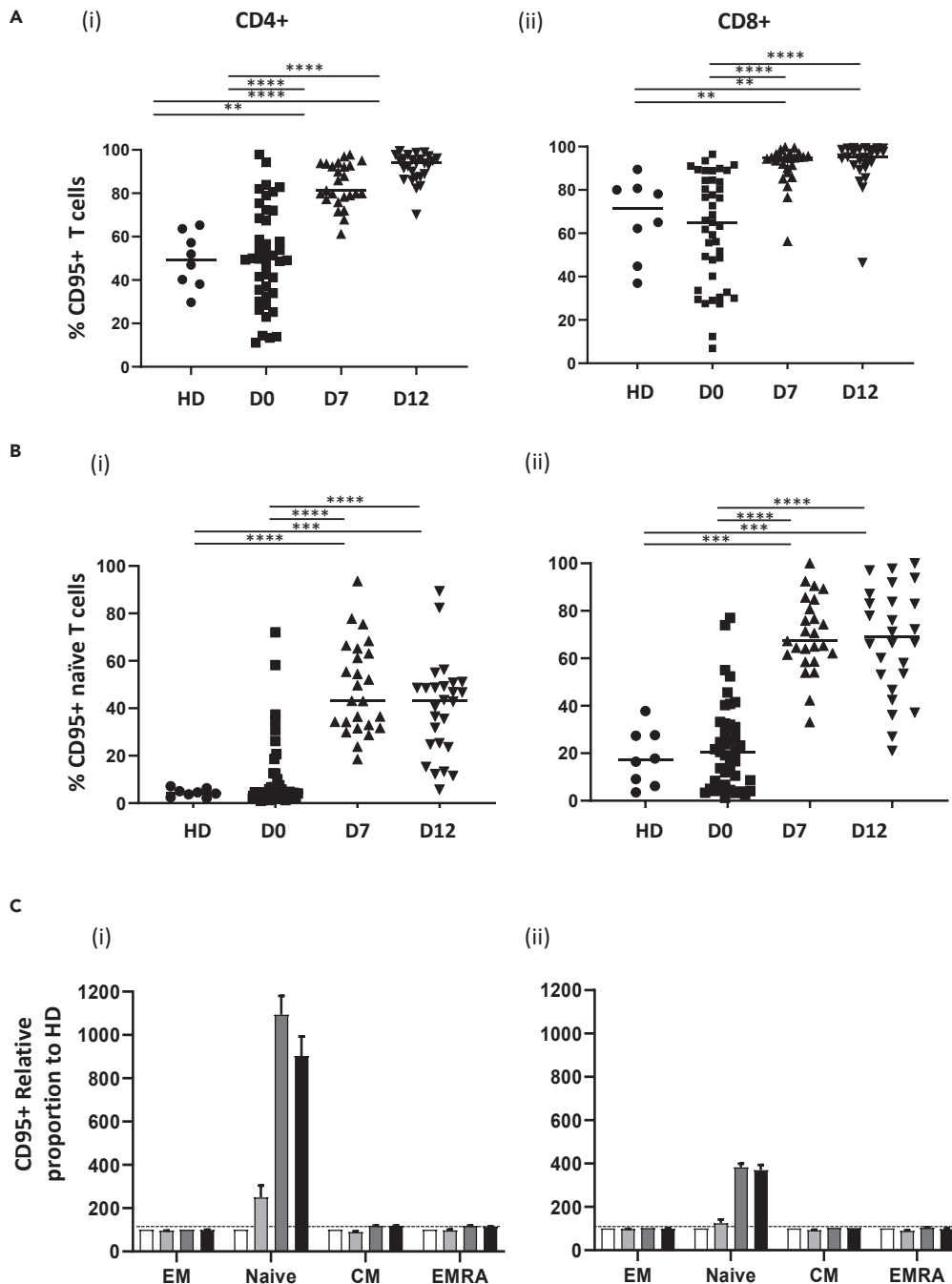
Figure 3. Fas expression is markedly upregulated on naive T cells during lymphopenia-induced proliferation

(A) Fas (CD95) expression on CD4+ (i) and CD8+ (ii) T cells in healthy donors (HD, n = 8) and in patients at day 0 (D0, n = 41), Day 7 (D7, n = 25) and day 12 (D12, n = 26) post-transplant.

(B) Proportion of naive CD4+ (i) and naive CD8+ (ii) T cells expressing CD95 in healthy donors (HD, n = 8) and in patients at D0 (n = 41), D7 (n = 25) and D12 (n = 26) post-transplant.

(C) Mean proportion of CD4+ and CD8+ T cell subsets expressing CD95 in patient samples relative to healthy donors (where HD = 100% represented as dotted line) in CD4+ (i) and CD8+ (ii) T cells (HD; white bars, D0; light gray bars, WK1; dark gray bars, WK2; black bars). Error bars depict standard error mean (SEM). Kruskal-Wallis with Dunn's multiple comparison test was performed, **p < 0.01, ***p < 0.001, ****p < 0.0001.

IL-7R expression fell markedly during the first two weeks post-autograft in both the CD4+ and CD8+ T cell pools. Indeed, the proportion of IL-7R-positive cells decreased by around 50% in both subsets, albeit from a slightly higher starting level of 82% in CD4+ populations compared to 68% in the CD8+ pool (Figure 4A). In contrast, IL-2Rα expression was seen to be increased in both subsets, particularly in the CD4+ pool. Within CD4+ cells, values rose 5-fold, from 3.6% on day 0–19% at day 12, whilst the percentage increase was from 0.1% to 1%, respectively, within the CD8+ population (Figure 4B).

We next examined the expression of IL-7R and IL-2Rα on naive, central memory, effector, and effector memory pools compared to healthy donors. IL-7R expression fell on all memory subsets during the first 2 weeks, and this was particularly marked on EMs (Figure 4C). In contrast, IL-2Rα expression increased during this period, most particularly within the naive pool where the proportion of CD25 + cells increased by 4.7 and 3.6-fold, respectively, in the CD4+ and CD8+ repertoires (Figure 4D).

LIP favors expansion of regulatory CD4+ and CD8+ T cells

Downregulation of IL-7 (CD127) and high levels of IL-2Rα (CD25) are characteristic features of regulatory T cells (Liu et al., 2006). As such we were next interested to assess if T cells were driven toward a regulatory phenotype during LIP. Tregs were identified by the phenotype CD25 + CD127-FOXP3+ within the CD4+ and CD8+ T cell population. The percentage of CD4+ Tregs was 8.3% at day 12, nearly double the value of 4.2% in HD (Figure 5A). FoxP3+ CD8+ T cells were not detected (data not shown). FOXP3+ CD4+ T cells were more proliferative than FOXP3- CD4+ T cells at D12 post-transplant as shown by Ki67 + staining (Figure S2). There was an increase in FOXP3+ CD4+ T cells at D12 compared to D0 (Figure S3), but there was no significant difference between percentage apoptotic or percentage live CD25 + CD4+ T cells between D0 and D12 post-transplant (Figure S2). In addition, we also interrogated the transcriptional profile of T EM populations at day 12 compared to EMs from healthy donors. Gene set enrichment analysis (GSEA) showed strong correlations between gene expression in EMs at day 12 and a range of data sets from activated Tregs subsets (Figure 5B). Indeed, a wide range of individual genes that are differentially expressed in Tregs were seen to exhibit a similar profile in day 12 EMs (Figure 5C). Barcode plots from gene set enrichment analysis further confirmed the correlation of day 12 transcriptional signature with that reported in T regulatory subsets, particularly in relation to the profile of downregulated genes (Figure 5D).

Transcriptional profiling identifies signaling pathways that drive LIP

In order to investigate the biochemical basis for LIP, we further interrogated transcriptional analysis of FACS-sorted CD4+ and CD8+ T EMs (CD45RA-CCR7-) from patients at day 12 compared to those from healthy donors. Principal component analysis (PCA) and hierarchical clustering analysis revealed discrete clustering of CD4+ and CD8+ populations from patients or healthy donors with PC1 axis separating D12 from HD and PC2 axis separating CD4 from CD8 subsets (Figures 6A and S4). Greater transcriptional differences were present between CD4+ and CD8+ T cells at D12 compared to HD indicating some differential mechanisms of acute LIP between these two subsets (Figure S4). Indeed, nearly twice as many genes exhibited LIP-driven differential expression within CD8+ subsets compared to CD4+ cells (2361 and 1238, respectively) and downregulation of gene expression was around two-fold more common than upregulation in both subsets (Figures 6B and 6C). Eight hundred ninety four genes were differentially regulated in both the CD4+ and CD8+ signatures, whereas expression of 333 and 1450 genes was uniquely modulated in either CD4+ or CD8+ cells, respectively (Figure 6D). Alignment of individual genes allowed detection of the most strongly upregulated or downregulated genes in the 'CD4+CD8', 'CD4-only', and 'CD8-only' transcriptional profiles in order to facilitate study of shared and differential responses to LIP in CD4 and CD8 subsets. Genes most strongly upregulated in both subsets included Tubulin 6 (TUBB6), which is known to play a role in reorganization of the cytoskeleton during division and migration of immune cells (Sumoza-Toledo and Santos-Argumedo, 2004); CBS, a molecule involved in the biosynthesis of hydrogen sulfide which is a strong enhancer of T cell activation (Miller et al., 2012) and the serine threonine kinase STK33. Strongly downregulated genes in both subsets included the metalloprotease domain containing ADAM23, adhesion molecule SDK2, and sphingosine 1-phosphate receptor S1PR5. Modulation of Sphingosine 1-phosphate signaling is of particular note given its important role in directing T cell migration between lymphoid organs and circulatory fluids (Baeyens et al., 2015). Subset-specific gene expression changes of particular interest include downregulation of the CD6 ligand CDCP1 and the innate immune receptor for self LILRB1 on CD4 cells. Wnt/β-catenin signaling is required for the suppression of terminal differentiation and is essential for T cell memory formation (Gattinoni et al., 2010) and interestingly we observe strong increased expression in the Wnt/β-catenin signaling regulator molecule SFRP4 in the CD8-only subset.
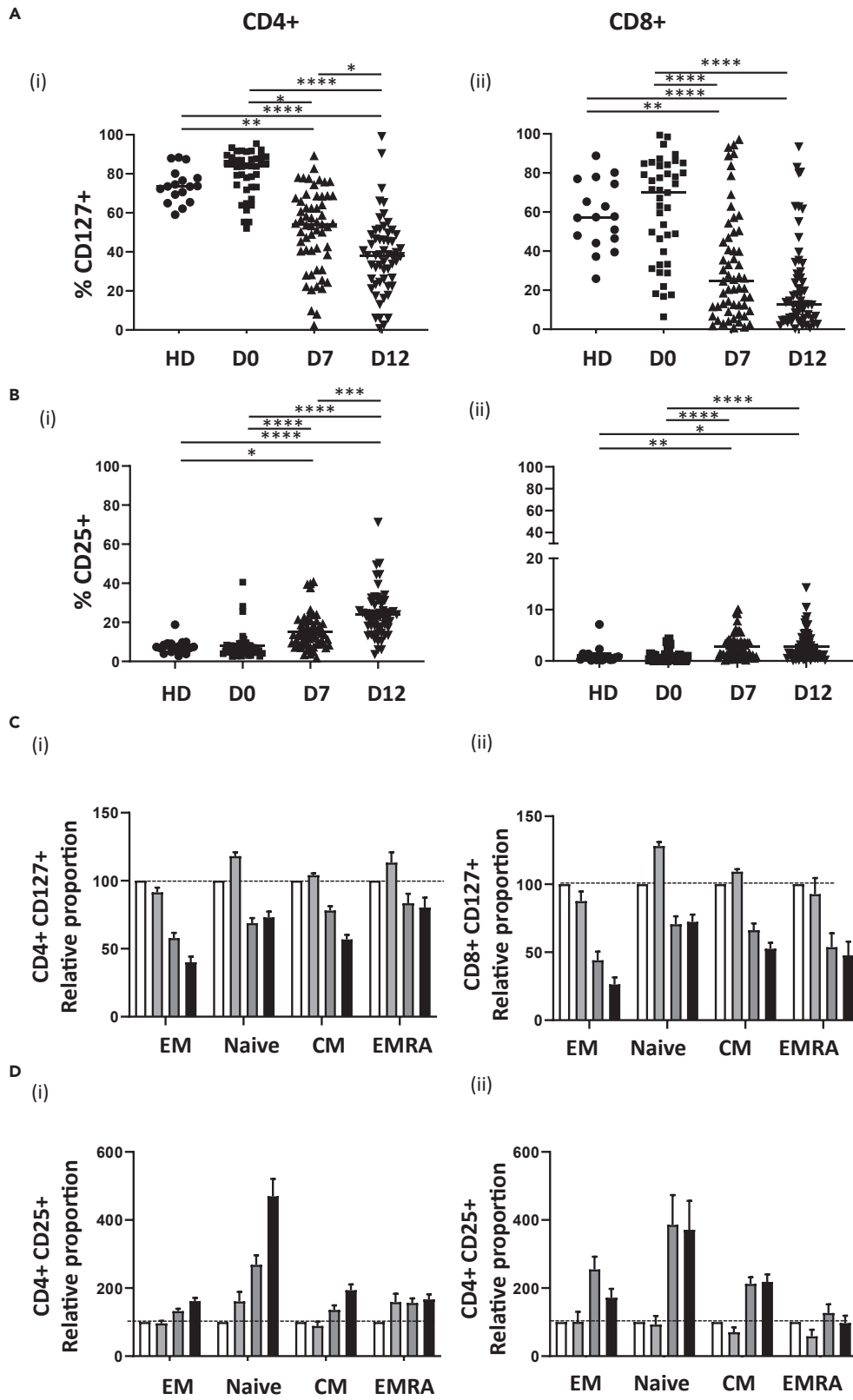
A

CD4+

(i)

CD8+

(ii)

B

(i)

(ii)

C

(i)

(ii)

D

(i)

(ii)

Figure 4. Reciprocal pattern of expression of IL-7R and IL-2Rα during lymphopenia-induced proliferation

CD127 (A) and CD25 staining (B) on CD4+ (i) and CD8+ (ii) T cells from healthy donors (HD, n = 17) and autograft patients at day 0 (D0, n = 41) and day 7 (D7, n = 57) and day 12 (D12, n = 56) post-transplant. The mean proportion of CD4+ and CD8+ T cell subsets expressing CD127 and CD25 was calculated for healthy donors (n = 17) and patients at day 0 (n = 41), D7 (n = 57) and D12 (n = 56) post-transplant.

The percentage expression for the patient samples at the three time points was then calculated relative to HD (where HD = 100%) for CD127 (C) and CD25 (D) on CD4+ (i) and CD8+ (ii) T cells (HD; white bars, D0; light gray bars, D7; dark gray bars, D12; black bars). Error bars depict standard error mean (SEM). Kruskal-Wallis with Dunn's multiple comparison test was performed, *p < 0.05, **p < 0.01, ***p < 0.001, ****p < 0.0001.

GSEA of selected MSigDB hallmark gene sets identified a wide range of upregulated pathways including oxidative phosphorylation and transcriptional targets of *E2F* and *MYC* (Figures 7A and S5). A strong proliferative profile was seen in LIP cells with activation of the nutrient sensor mTORC1 pathway and PI3/Akt signaling. Of note, genes associated with fatty acid metabolism were strikingly increased although the glycolysis pathway was increased in CD8+ cells only. Pathways associated with interferon-α and interferon-γ signaling were both activated whilst genes associated with TNF-α and TGF-β signaling were strongly downregulated during LIP (Figure 7B). Analysis of the JAK/STAT signaling pathway revealed differential expression of many genes, including upregulation of *JAK2* but reduced expression of *STAT3* and *STAT4* during LIP (Figure 7C). Transcription factor pathway analysis showed that genes regulated by NRSF were upregulated during LIP. Finally, many miRNA-target gene sets were downregulated (Figure S6) and overall a substantial proportion of non-coding RNA molecules were differentially expressed during LIP (Figure S7).

DISCUSSION

Homeostatic processes maintain the peripheral lymphocyte count at a remarkably stable level across the lifecourse. LIP acts to sustain lymphoid numbers and as chemotherapy-induced LIP is an essential component of almost all current CAR-T regimens we were interested to examine the mechanisms that regulate this process.

T cell proliferation was seen to increase very early after chemotherapy and the T cell count increased to around 26,000/mL at day 12 post-transplant driven by extensive cell division and Ki-67 expression on 50% of cells. CD4+ and CD8+ T cell populations expanded at equal rates over the first two weeks post-transplant (Tan et al., 2002).

A striking feature was the collapse in the percentage of naive cells in the early post-transplant period as these were replaced by an effector T cell pool, and no signature of CD31 + recent thymic emigrants was seen in this early period (Figure S8). This finding supports observations in murine systems that LIP drives naive cells to undergo activation, including acquisition of short-term functional capacity (Murali-Krishna and Ahmed, 2000). The survival of naive T cells requires their continuous contact with self-peptide:MHC ligands (Murali-Krishna et al., 1999) and LIP appears to further drive this process into T cell activation. Indeed the enrichment of auto-reactive cells and clinical development of auto-immune disease is well recognized during homeostatic proliferation (Jones et al., 2009) (King et al., 2004).

IL-7 is the major rheostat of LIP (Bourgeois and Stockinger, 2006) (Guimond et al., 2009) and IL-7R (CD127) expression fell on all T cell memory subsets during LIP, including the naive pool. However, IL-7 signaling may not be the only mechanism leading to CD127 downregulation as this can also be observed following TCR signaling (Carrette and Surh, 2012). Interestingly, this decrease was mirrored by a comparable, albeit smaller, increase in IL-2Rα (CD25) expression and likely reflects reciprocal regulation of these receptors. This was most clearly observed within the naive T cell pool where a 4-fold increase in CD25 expression was observed compared to baseline. Of note, IL-7 directly increases expression of the IL-2Rα (Simonetta et al., 2014) and is the likely mechanism to explain this observation.

This IL-7R^low IL-2Rα^high phenotype is characteristic of regulatory T cells and we were therefore interested to determine the profile of regulatory T cells during LIP. Importantly, the proportion of FoxP3+CD4+ regulatory cells was seen to double to reach over 8% of the CD4+ T cell pool. Similar findings have been observed in the months following alemtuzumab therapy (Bloom et al., 2008) and in murine models (Bosco et al., 2006). Tregs have a high endogenous proliferation rate and expand preferentially after adoptive transfer (Fisson et al., 2003) (Tang et al., 2008). As such, this phenotypic and transcriptional data indicates that while there
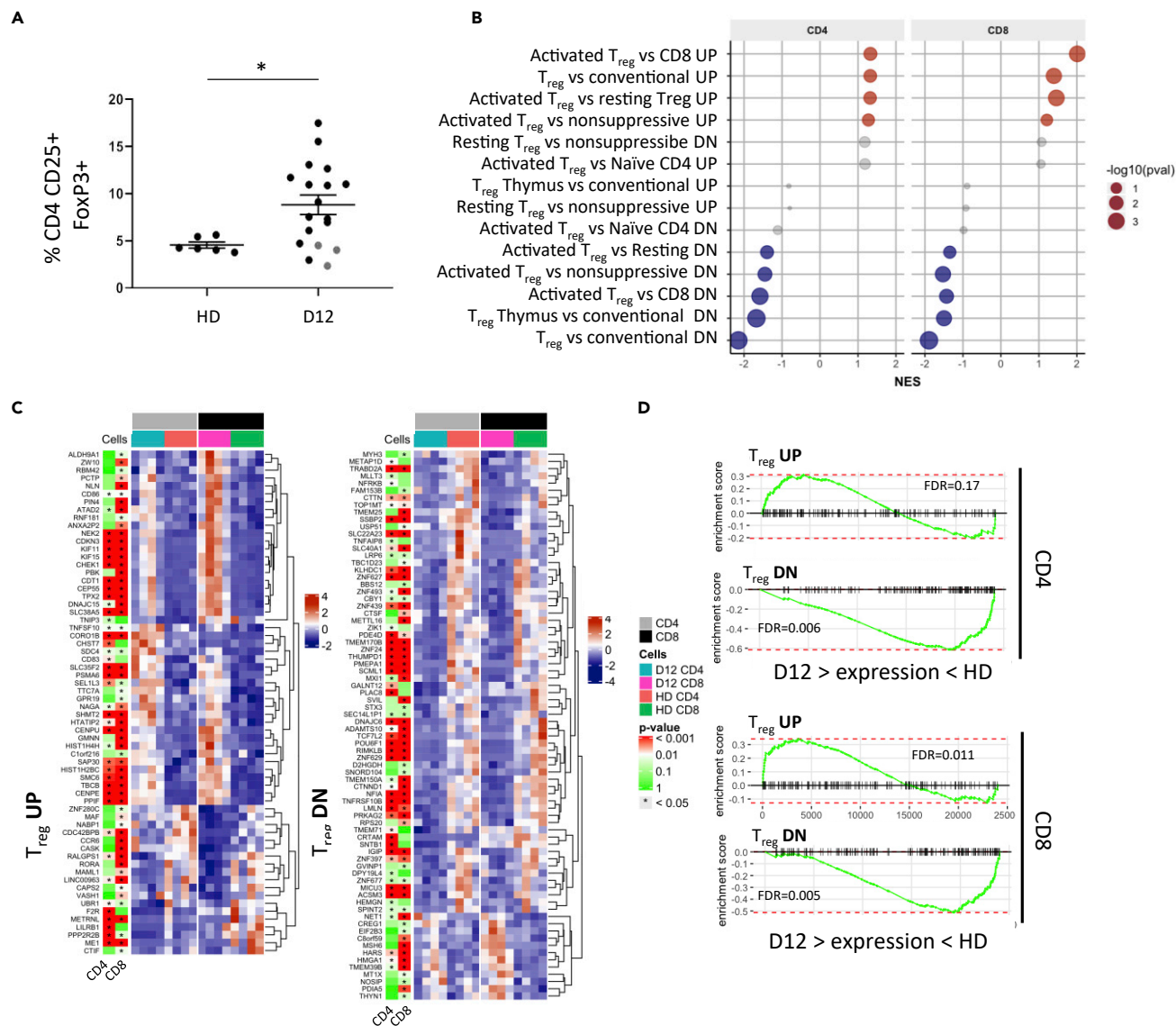
Figure 5. Lymphopenia-induced proliferation drives T cells toward a regulatory phenotype

(A) Proportion of CD4+CD25 + CD127-FoxP3+ T cells in healthy donors (HD n = 6) and autograft patients at day 12 post-transplant (n = 18) (*p = 0.023).

(B) Gene set enrichment analysis (GSEA) of relevant published T$_{reg}$ signature gene sets. RNA sequencing was performed on FACS-sorted CD45RA-CCR7- CD4 and CD8 effector T cells of healthy donor (HD; n = 4) and day 12 post-autograft patients (D12; n = 4). Differential expression analysis performed for D12 vs HD on CD4 and CD8 effector T cell subset data separately. GSEA results show normalized enrichment score (NES) for selected gene sets and colored circles indicate significant enrichments toward genes upregulated (Red) or downregulated (blue) in CD4/CD8 effector T cells at D12 compared to HD.

(C) Gene expression profiles of published signature genes (GSE22045 – genes UP/DN-regulated in T$_{reg}$ cells compared to conventional T cells) observed in FACS-sorted effector T cells at D12 compared to HD. Shown are genes from this gene set that are differentially expressed genes between D12 and HD in at least one cell type (CD4/CD8). p values are from differential expression analysis of D12 vs HD CD4/CD8 and are adjusted for multiple testing. Color key = standard deviation from the mean normalized expression level.

(D) Barcode plots from gene set enrichment analysis of gene sets in C showing enrichments on the fold change expression ranking from D12 vs HD differential expression analysis.

does not seem to be a survival advantage, there is selective global expansion of regulatory T cells post-transplant during LIP. TGF-β levels were markedly suppressed at day 12 after transplant and transcription activity associated with TGF-β signaling was strongly downregulated. As such, it appears unlikely that this reflects TGF-β-mediated peripheral conversion of EMs. Rather we suggest that homeostatic cytokines can themselves initiate partial regulatory conversion during LIP. Depletion of Treg populations can augment
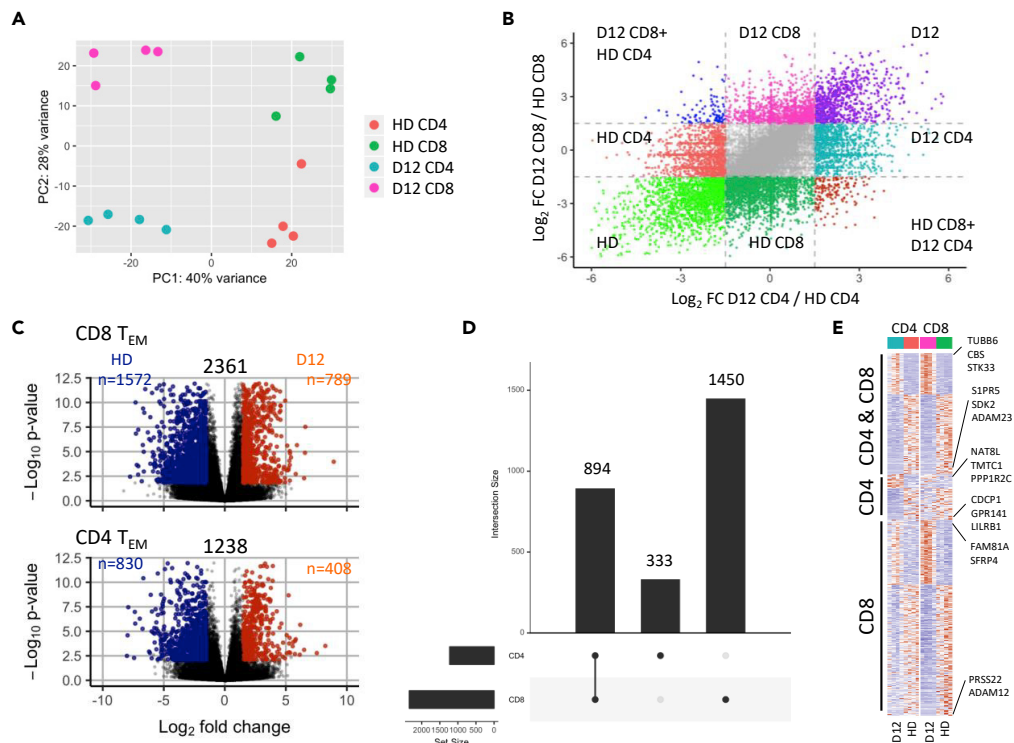
Figure 6. Transcriptional profiling of effector T cells during lymphopenia-induced proliferation

(A) Transcriptomes of FACS-sorted CD45RA-CCR7- CD4 and CD8 effector T cells of healthy donor and day 12 post-autograft patients in reduced dimensional space. Principal component coordinates generated by principal component analysis on normalized gene count data from RNA sequencing.

(B) Overview of gene-level transcriptional changes from calculated fold changes in gene expression at day 12 compared to HD for CD4 and CD8 effector T cells.

(C) Differential expression analysis results from D12 vs HD comparisons of CD4 and CD8 cells. Colored points indicate differentially expressed genes in the comparison (Orange = UP at D12; Blue = DOWN at D12). Genes are deemed to differentially expressed if adjusted p value <0.05 and absolute log2FC > 1.5.

(D and E) (D) Overlaps of differentially expressed genes between CD4 and CD8 cells (E) Gene expression profiles of differentially expressed genes from C. Color indicates standard deviation from mean (red = increase at D12; blue = decrease at D12). Genes are grouped into those identified as differentially expressed between D12 and HD samples in both CD4 and CD8, CD4-only or CD8-only effector T cells. The top three UP/DN differentially expressed genes in each group (ordered by fold change) are labeled.

tumor-specific immune responses in murine models (Baba et al., 2012) (Saida et al., 2015) and as such our findings suggest that a similar approach may potentially act to further boost tumor-specific immune responses after autograft (North, 1982) or CAR-T infusion. Further, these data may guide improvement of strategies for altered expression of these cytokines and/or their cognate receptors in CAR T cells to enhance the persistence and thereby antitumor activity of these engineered cells (Yao et al., 2012) (Andersen et al., 2016). Clearly, this approach must be titrated carefully in order to limit potential auto-immune reactions (King et al., 2004) and Treg may also play a role in supporting clonal diversity of EMs during LIP (Winstead et al., 2010) (Bolton et al., 2015)

One of the most interesting observations was remarkable increase in Fas (CD95) expression on T cells during LIP. Fas is a marker of T cell engagement and was, as expected, expressed exclusively on effector/memory pools prior to transplant in keeping with its role as a major regulator of lymphoid survival. However, Fas became expressed on the majority of 'phenotypically naïve' populations and reveals that LIP induces human naive cells to undergo partial T cell activation, presumably through recognition of self-peptides presented by HLA (Hsieh et al., 2004) (Johnson and Jameson, 2010). It is interesting to speculate why naive T cells undergo activation on self-peptides during LIP. As discussed above, naive cells utilize engagement with self-peptide:MHC for survival but although TCR signaling is attenuated by high phosphatase
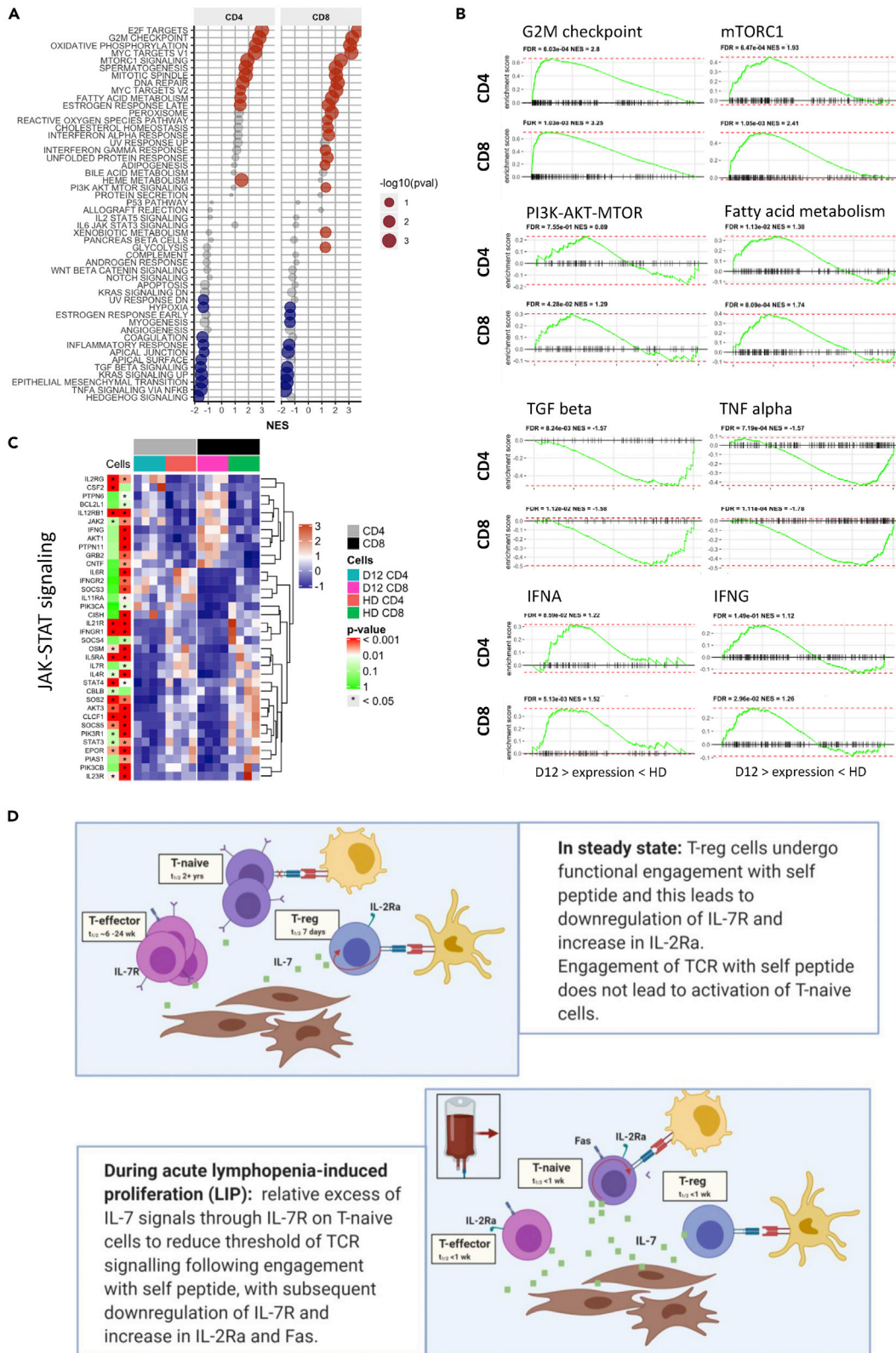
A

B

C

JAK-STAT signaling

D

In steady state: T-reg cells undergo functional engagement with self peptide and this leads to downregulation of IL-7R and increase in IL-2Ra.
Engagement of TCR with self peptide does not lead to activation of T-naive cells.

During acute lymphopenia-induced proliferation (LIP): relative excess of IL-7 signals through IL-7R on T-naive cells to reduce threshold of TCR signalling following engagement with self peptide, with subsequent downregulation of IL-7R and increase in IL-2Ra and Fas.

Figure 7. Effector T cells during lymphopenia-induced proliferation are undergoing fatty acid metabolism, show signatures of increased IFNA, IFNG, mTORC, and PI3K response and reduced TGFbeta and TNFalpha response compared to healthy donor

(A) GSEA of selected MSigDB Hallmark gene sets. Shown are selected sets having FDR <0.2 in either CD4 or CD8 D12 vs HD comparisons. Colored circles indicate a significant enrichments (FDR<0.1) toward genes upregulated (Red) or downregulated (blue) at D12 compared to HD.

(B) Selected significantly enriched gene sets from A including genes upregulated in G2M transition (cell-cycle progression) and fatty acid metabolism and in response to stimulation of the signaling pathways IFNA, IFNG, TGF beta, and TNF alpha. FDR = false discovery rate; NES = normalized enrichment score.

(C) Gene expression profiles of UP/DN-regulated JAK-STAT signaling pathway genes in effector T cells at D12 post-autograft (D12) compared to healthy donors (HD). Showing D12 vs HD differentially expressed genes (in at least one cell type). p values are from differential expression analysis of D12 vs HD samples for each cell type and are adjusted for multiple testing. Color key = standard deviation from the mean normalized expression level.

(D) Schematic diagram representing mechanisms of cytokine-driven T cell proliferation during LIP. Created using Biorender.

expression (Cho et al., 2016) they remain highly sensitive to cytokine-mediated activation and it thus seems that the supra-physiological levels of IL-7 during LIP serve to trigger partial T cell activation.

Chemotherapy-induced LIP is clearly not a natural event but observations from extreme phenotypes can provide insights into immune regulation and our findings may have implications for regulation of the physiological regulatory T cell pool which is characterized by high levels of proliferation (Vukmanovic-Stejic et al., 2006), IL-7R^{low}IL-2Rα^{high} phenotype and recognition of self-peptide (Cozzo et al., 2003). It is now clear that Tregs are strongly dependent on peripheral IL-7 engagement (Bayer et al., 2008) (Simonetta et al., 2012) (Kim et al., 2012) (Bayer et al., 2008), and these data therefore suggest that many of the features of physiological Treg cells are themselves driven by enhanced sensitivity to homeostatic cytokines.

Differential expression of a wide variety of genes was observed during LIP, and it was noteworthy that many of these defined selective processes within either CD4+ or CD8+ lineages. However, 894 transcripts underwent similar regulation within both subsets and may represent targets for future T cell engineering in order to facilitate 'chemotherapy-free' T cell expansion without inducing LIP. Genes associated with fatty acid metabolism were highly upregulated and IL-7 induces T cell expression of glycerol channel aquaporin 9 (AQP9) and promotes glycerol import for fatty acid esterification and triglyceride (TAG) synthesis (Cui et al., 2015) (Barra et al., 2010). However AQP9 expression was not increased during LIP although expression of genes such as *AGPS, GNPAT* and *TPI1* that encode enzymes that catalyze reactions converting DHAP for lipid biosynthesis was strongly increased.

Genes associated with IFN-α signaling were also strongly upregulated, with a more modest increase in IFN-γ transcriptional activity. mTORC1 transcription, a major rheostat of cellular energy signaling, was also strongly increased. An unexpected finding was strong transcriptional downregulation of the TGF-β pathway. TGF-β is a major negative regulator of IL-7 driven T cell proliferation (Nguyen and Sieg, 2017), but serum levels are low in the early post-transplant period (Kyrcz-Krzemien et al., 2011). TGF-β RII expression was downregulated in both CD4 and CD8 T cells, whilst expression of KLF10, a key transcriptional regulator of TGF-β RII(Papadakis et al., 2015) is increased. Inhibition of TGF-β signaling through expression of a dominant negative TGF-β RII strongly boosts the T cell memory pool (Lucas et al., 2000) and is being used as a mechanism to facilitate adoptive T cell expansion without the need for pre-conditioning therapy (Bollard et al., 2018). Several transcription factors were differentially regulated during LIP, including c-MYB, which acts to maintain the stem cell memory pool (Gautam et al., 2019), and the expression of genes upregulated by NRSF was also increased by day 12.

This comprehensive characterization of acute LIP within the human lymphoid system reveals remarkable levels of proliferation driven by homeostatic cytokines and TCR-mediated activation of naive cells. Furthermore, a shift toward a 'regulatory' IL-7R^{low}IL-25Ra^{high} phenotype and transcriptional profile is observed across the whole repertoire and supports growing interest in IL-7 as a major regulator of Treg phenotype in health and disease. This increase in regulatory phenotype may underpin the utility of autograft transplantation in the management of auto-immune conditions but also suggests opportunities for therapeutic depletion in the setting of malignancy disease. These observations may also facilitate novel therapeutic opportunities to simplify conditioning regimens for patients undergoing adoptive T cell therapy.

Limitations of the study

Chemotherapy-induced lymphopenia is not a natural phenomenon in humans but provides a setting to study the proliferative immune response to lymphopenia *in vivo*. A caveat of our study is that gene expression patterns were studied at the cell population level by bulk RNA sequencing, and it will be of interest in

future studies to assess immune cells at the single cell level to further understand cellular heterogeneity and gene expression dynamics induced by the lymphopenic environment.

Resource availability

Lead contact

Further information and requests for resources and data should be directed to the lead contact, Paul Moss, Institute of Immunology and Immunotherapy, University of Birmingham, Birmingham, UK (P.Moss@bham.ac.uk).

Materials availability

This study did not generate new unique reagents.

Data and code availability

The RNA sequencing data in this paper have been deposited in GEO:GSE150834 (https://www.ncbi.nlm.nih.gov/geo/query/acc.cgi?acc=GSE150834).

METHODS

All methods can be found in the accompanying Transparent Methods supplemental file.

SUPPLEMENTAL INFORMATION

Supplemental information can be found online at https://doi.org/10.1016/j.isci.2021.102164.

AUTHORS CONTRIBUTION

S.E. and P.M. conceptualized the study; S.E., T.R., K.V., and H.C. performed the experiments; T.R., C.S., H.C., and F.K. performed sample collection, processing and storage; F.K., J.N., and R.M. consented patients to the study and collected patient samples; S.E. and K.V. analyzed the data from flow cytometry and ELISA; and W.C. analyzed the sequencing data; S.E., K.V., W.C., J.Z., and P.M. contributed in interpretation of the data; S.E., K.V., W.C., and P.M. wrote the paper; J.Z. helped to review and edit the paper. All authors read and approved the final manuscript.

DECLARATION OF INTERESTS

The authors declare that there is no conflict of interest.

REFERENCES

Andersen, R., Donia, M., Ellebaek, E., Borch, T.H., Kongsted, P., Iversen, T.Z., Hölmich, L.R., Hendel, H.W., Met, Ö., Andersen, M.H., et al. (2016). Long-lasting complete responses in patients with metastatic melanoma after adoptive cell therapy with tumor-infiltrating lymphocytes and an attenuated IL2 regimen. Clin. Cancer Res. *22*, 3734.

Baba, J., Watanabe, S., Saida, Y., Tanaka, T., Miyabayashi, T., Koshio, J., Ichikawa, K., Nozaki, K., Koya, T., Deguchi, K., et al. (2012). Depletion of radio-resistant regulatory T cells enhances antitumor immunity during recovery from lymphopenia. Blood *120*, 2417–2427.

Baeyens, A., Fang, V., Chen, C., and Schwab, S.R. (2015). Exit strategies: S1P signaling and T cell migration. Trends Immunol. *36*, 778–787.

Barra, N.G., Reid, S., Mackenzie, R., Werstuck, G., Trigatti, B.L., Richards, C., Holloway, A.C., and Ashkar, A.A. (2010). Interleukin-15 contributes to the regulation of murine adipose tissue and human adipocytes. Obesity (Silver Spring) *18*, 1601–1607.

Bayer, A.L., Lee, J.Y., De La Barrera, A., Surh, C.D., and Malek, T.R. (2008). A function for IL-7R for CD4+CD25+Foxp3+ T regulatory cells. J. Immunol. *181*, 225–234.

Bloom, D.D., Chang, Z., Fechner, J.H., Dar, W., Polster, S.P., Pascual, J., Turka, L.A., and Knechtle, S.J. (2008). CD4+ CD25+ FOXP3+ regulatory T cells increase de novo in kidney transplant patients after immunodepletion with Campath-1H. Am. J. Transpl. *8*, 793–802.

Bollard, C.M., Tripic, T., Cruz, C.R., Dotti, G., Gottschalk, S., Torrano, V., Dakhova, O., Carrum, G., Ramos, C.A., Liu, H., et al. (2018). Tumor-specific T-cells engineered to overcome tumor immune evasion induce clinical responses in patients with relapsed hodgkin lymphoma. J. Clin. Oncol. *36*, 1128–1139.

Bolton, H.A., Zhu, E., Terry, A.M., Guy, T.V., Koh, W.P., Tan, S.Y., Power, C.A., Bertolino, P., Lahl, K., Sparwasser, T., et al. (2015). Selective Treg reconstitution during lymphopenia normalizes DC costimulation and prevents graft-versus-host disease. J. Clin. Invest. 125, 3627–3641.

Bosco, N., Agenes, F., Rolink, A.G., and Ceredig, R. (2006). Peripheral T cell lymphopenia and concomitant enrichment in naturally arising regulatory T cells: the case of the pre-Talpha gene-deleted mouse. J. Immunol. 177, 5014–5023.

Bourgeois, C., and Stockinger, B. (2006). CD25+CD4+ regulatory T cells and memory T cells prevent lymphopenia-induced proliferation of naive T cells in transient states of lymphopenia. J. Immunol. 177, 4558–4566.

Brentjens, R.J., Davila, M.L., Riviere, I., Park, J., Wang, X., Cowell, L.G., Bartido, S., Stefanski, J., Taylor, C., Olszewska, M., et al. (2013). CD19-targeted T cells rapidly induce molecular remissions in adults with chemotherapy-refractory acute lymphoblastic leukemia. Sci. Transl Med. 5, 177ra38.

Carrette, F., and Surh, C.D. (2012). IL-7 signaling and CD127 receptor regulation in the control of T cell homeostasis. Semin. Immunol. 24, 209–217.

Cho, J.H., Kim, H.O., Ju, Y.J., Kye, Y.C., Lee, G.W., Lee, S.W., Yun, C.H., Bottini, N., Webster, K., Goodnow, C.C., et al. (2016). CD45-mediated control of TCR tuning in naive and memory CD8(+) T cells. Nat. Commun. 7, 13373.

Condomines, M., Veyrune, J.L., Larroque, M., Quittet, P., Latry, P., Lugagne, C., Hertogh, C., Kanouni, T., Rossi, J.F., and Klein, B. (2010). Increased plasma-immune cytokines throughout the high-dose melphalan-induced lymphodepletion in patients with multiple myeloma: a window for adoptive immunotherapy. J. Immunol. 184, 1079–1084.

Cozzo, C., Larkin, J., 3rd, and Caton, A.J. (2003). Cutting edge: self-peptides drive the peripheral expansion of CD4+CD25+ regulatory T cells. J. Immunol. 171, 5678–5682.

Cui, G., Staron, M.M., Gray, S.M., Ho, P.C., Amezquita, R.A., Wu, J., and Kaech, S.M. (2015). IL-7-Induced glycerol transport and TAG synthesis promotes memory CD8+ T cell longevity. Cell 161, 750–761.

Fisson, S., Darrasse-Jeze, G., Litvinova, E., Septier, F., Klatzmann, D., Liblau, R., and Salomon, B.L. (2003). Continuous activation of autoreactive CD4+ CD25+ regulatory T cells in the steady state. J. Exp. Med. 198, 737–746.

Francois, B., Jeannet, R., Daix, T., Walton, A.H., Shotwell, M.S., Unsinger, J., Monneret, G., Rimmele, T., Blood, T., Morre, M., et al. (2018). Interleukin-7 restores lymphocytes in septic shock: the IRIS-7 randomized clinical trial. JCI Insight 3, e98960.

Gattinoni, L., Finkelstein, S.E., Klebanoff, C.A., Antony, P.A., Palmer, D.C., Spiess, P.J., Hwang, L.N., Yu, Z., Wrzesinski, C., Heimann, D.M., et al. (2005). Removal of homeostatic cytokine sinks by lymphodepletion enhances the efficacy of adoptively transferred tumor-specific CD8+ T cells. J. Exp. Med. 202, 907–912.

Gattinoni, L., Ji, Y., and Restifo, N.P. (2010). Wnt/beta-catenin signaling in T-cell immunity and cancer immunotherapy. Clin. Cancer Res. : official J. Am. Assoc. Cancer Res. 16, 4695–4701.

Gautam, S., Fioravanti, J., Zhu, W., Le Gall, J.B., Brohawn, P., Lacey, N.E., Hu, J., Hocker, J.D., Hawk, N.V., Kapoor, V., et al. (2019). The transcription factor c-Myb regulates CD8(+) T cell stemness and antitumor immunity. Nat. Immunol. 20, 337–349.

Goldrath, A.W., Bogatzki, L.Y., and Bevan, M.J. (2000). Naive T cells transiently acquire a memory-like phenotype during homeostasis-driven proliferation. J. Exp. Med. 192, 557–564.

Guimond, M., Veenstra, R.G., Grindler, D.J., Zhang, H., Cui, Y., Murphy, R.D., Kim, S.Y., Na, R., Hennighausen, L., Kurtulus, S., et al. (2009). Interleukin 7 signaling in dendritic cells regulates the homeostatic proliferation and niche size of CD4+ T cells. Nat. Immunol. 10, 149–157.

Hsieh, C.S., Liang, Y., Tyznik, A.J., Self, S.G., Liggitt, D., and Rudensky, A.Y. (2004). Recognition of the peripheral self by naturally arising CD25+ CD4+ T cell receptors. Immunity 21, 267–277.

Johnson, L.D., and Jameson, S.C. (2010). Self-specific CD8+ T cells maintain a semi-naive state following lymphopenia-induced proliferation. J. Immunol. 184, 5604–5611.

Jones, J.L., Phuah, C.L., Cox, A.L., Thompson, S.A., Ban, M., Shawcross, J., Walton, A., Sawcer, S.J., Compston, A., and Coles, A.J. (2009). IL-21 drives secondary autoimmunity in patients with multiple sclerosis, following therapeutic lymphocyte depletion with alemtuzumab (Campath-1H). J. Clin. Invest. 119, 2052–2061.

Kim, G.Y., Ligons, D.L., Hong, C., Luckey, M.A., Keller, H.R., Tai, X., Lucas, P.J., Gress, R.E., and Park, J.H. (2012). An in vivo IL-7 requirement for peripheral Foxp3+ regulatory T cell homeostasis. J. Immunol. 188, 5859–5866.

King, C., Ilic, A., Koelsch, K., and Sarvetnick, N. (2004). Homeostatic expansion of T cells during immune insufficiency generates autoimmunity. Cell 117, 265–277.

Kyrcz-Krzemien, S., Helbig, G., Zielinska, P., and Markiewicz, M. (2011). The kinetics of mRNA transforming growth factor beta1 expression and its serum concentration in graft-versus-host disease after allogeneic hemopoietic stem cell transplantation for myeloid leukemias. Med. Sci. Monit. 17, CR322–CR328.

Liu, W., Putnam, A.L., Xu-Yu, Z., Szot, G.L., Lee, M.R., Zhu, S., Gottlieb, P.A., Kapranov, P., Gingeras, T.R., Fazekas De St Groth, B., et al. (2006). CD127 expression inversely correlates with FoxP3 and suppressive function of human CD4+ T reg cells. J. Exp. Med. 203, 1701–1711.

Lucas, P.J., Kim, S.J., Melby, S.J., and Gress, R.E. (2000). Disruption of T cell homeostasis in mice expressing a T cell-specific dominant negative transforming growth factor beta II receptor. J. Exp. Med. 191, 1187–1196.

Mackall, C.L., and Gress, R.E. (1997). Pathways of T-cell regeneration in mice and humans: implications for bone marrow transplantation and immmunotherapy. Immunol. Rev. 157, 61–72.

Martin, C.E., Spasova, D.S., Frimpong-Boateng, K., Kim, H.O., Lee, M., Kim, K.S., and Surh, C.D. (2017). Interleukin-7 availability is maintained by a hematopoietic cytokine sink comprising innate lymphoid cells and T cells. Immunity 47, 171–182 e4.

Miller, T.W., Wang, E.A., Gould, S., Stein, E.V., Kaur, S., Lim, L., Amarnath, S., Fowler, D.H., and Roberts, D.D. (2012). Hydrogen sulfide is an endogenous potentiator of T cell activation. J. Biol. Chem. 287, 4211–4221.

Murali-Krishna, K., and Ahmed, R. (2000). Cutting edge: naive T cells masquerading as memory cells. J. Immunol. 165, 1733–1737.

Murali-Krishna, K., Lau, L.L., Sambhara, S., Lemonnier, F., Altman, J., and Ahmed, R. (1999). Persistence of memory CD8 T cells in MHC class I-deficient mice. Science 286, 1377–1381.

Nguyen, T.P., and Sieg, S.F. (2017). TGF-beta inhibits IL-7-induced proliferation in memory but not naive human CD4(+) T cells. J. Leukoc. Biol. 102, 499–506.

North, R.J. (1982). Cyclophosphamide-facilitated adoptive immunotherapy of an established tumor depends on elimination of tumor-induced suppressor T cells. J. Exp. Med. 155, 1063–1074.

Papadakis, K.A., Krempski, J., Reiter, J., Svingen, P., Xiong, Y., Sarmento, O.F., Huseby, A., Johnson, A.J., Lomberk, G.A., Urrutia, R.A., and Faubion, W.A. (2015). Krüppel-like factor KLF10 regulates transforming growth factor receptor II expression and TGF-β signaling in CD8+ T lymphocytes. Am. J. Physiol. Cell Physiol. 308, C362–C371.

Perales, M.A., Goldberg, J.D., Yuan, J., Koehne, G., Lechner, L., Papadopoulos, E.B., Young, J.W., Jakubowski, A.A., Zaidi, B., Gallardo, H., et al. (2012). Recombinant human interleukin-7 (CYT107) promotes T-cell recovery after allogeneic stem cell transplantation. Blood 120, 4882–4891.

Restifo, N.P., Dudley, M.E., and Rosenberg, S.A. (2012). Adoptive immunotherapy for cancer: harnessing the T cell response. Nat. Rev. Immunol. 12, 269–281.

Saida, Y., Watanabe, S., Tanaka, T., Baba, J., Sato, K., Shoji, S., Igarashi, N., Kondo, R., Okajima, M., Koshio, J., et al. (2015). Critical roles of chemoresistant effector and regulatory T cells in antitumor immunity after lymphodepleting chemotherapy. J. Immunol. 195, 726–735.

Simonetta, F., Gestermann, N., Bloquet, S., and Bourgeois, C. (2014). Interleukin-7 optimizes FOXP3+CD4+ regulatory T cells reactivity to interleukin-2 by modulating CD25 expression. PLoS One 9, e113314.

Simonetta, F., Gestermann, N., Martinet, K.Z., Boniotto, M., Tissieres, P., Seddon, B., and Bourgeois, C. (2012). Interleukin-7 influences FOXP3+CD4+ regulatory T cells peripheral homeostasis. PLoS One 7, e36596.

Sumoza-Toledo, A., and Santos-Argumedo, L. (2004). The spreading of B lymphocytes induced by CD44 cross-linking requires actin, tubulin, and vimentin rearrangements. J. Leukoc. Biol. 75, 233–239.

Takada, K., and Jameson, S.C. (2009). Naive T cell homeostasis: from awareness of space to a sense of place. Nat. Rev. Immunol. *9*, 823–832.

Tan, J.T., Ernst, B., Kieper, W.C., Leroy, E., Sprent, J., and Surh, C.D. (2002). Interleukin (IL)-15 and IL-7 jointly regulate homeostatic proliferation of memory phenotype CD8+ cells but are not required for memory phenotype CD4+ cells. J. Exp. Med. *195*, 1523–1532.

Tang, A.L., Teijaro, J.R., Njau, M.N., Chandran, S.S., Azimzadeh, A., Nadler, S.G., Rothstein, D.M., and Farber, D.L. (2008). CTLA4 expression

is an indicator and regulator of steady-state CD4+ FoxP3+ T cell homeostasis. J. Immunol. *181*, 1806–1813.

Vukmanovic-Stejic, M., Zhang, Y., Cook, J.E., Fletcher, J.M., Mcquaid, A., Masters, J.E., Rustin, M.H., Taams, L.S., Beverley, P.C., Macallan, D.C., and Akbar, A.N. (2006). Human CD4+ CD25hi Foxp3+ regulatory T cells are derived by rapid turnover of memory populations in vivo. J. Clin. Invest. *116*, 2423–2433.

Winstead, C.J., Reilly, C.S., Moon, J.J., Jenkins, M.K., Hamilton, S.E., Jameson, S.C., Way, S.S.,

and Khoruts, A. (2010). CD4+CD25+Foxp3+ regulatory T cells optimize diversity of the conventional T cell repertoire during reconstitution from lymphopenia. J. Immunol. *184*, 4749–4760.

Yao, X., Ahmadzadeh, M., Lu, Y.-C., Liewehr, D.J., Dudley, M.E., Liu, F., Schrump, D.S., Steinberg, S.M., Rosenberg, S.A., and Robbins, P.F. (2012). Levels of peripheral CD4+FoxP3+ regulatory T cells are negatively associated with clinical response to adoptive immunotherapy of human cancer. Blood *119*, 5688–5696.

Supplemental information

Lymphopenia-induced lymphoproliferation

drives activation of naive T cells

and expansion of regulatory populations

Eldershaw S, Verma K, Croft W, Rai T, Kinsella FAM, Stephens C, Chen H, Nunnick J, Zuo J, Malladi R, and Moss P
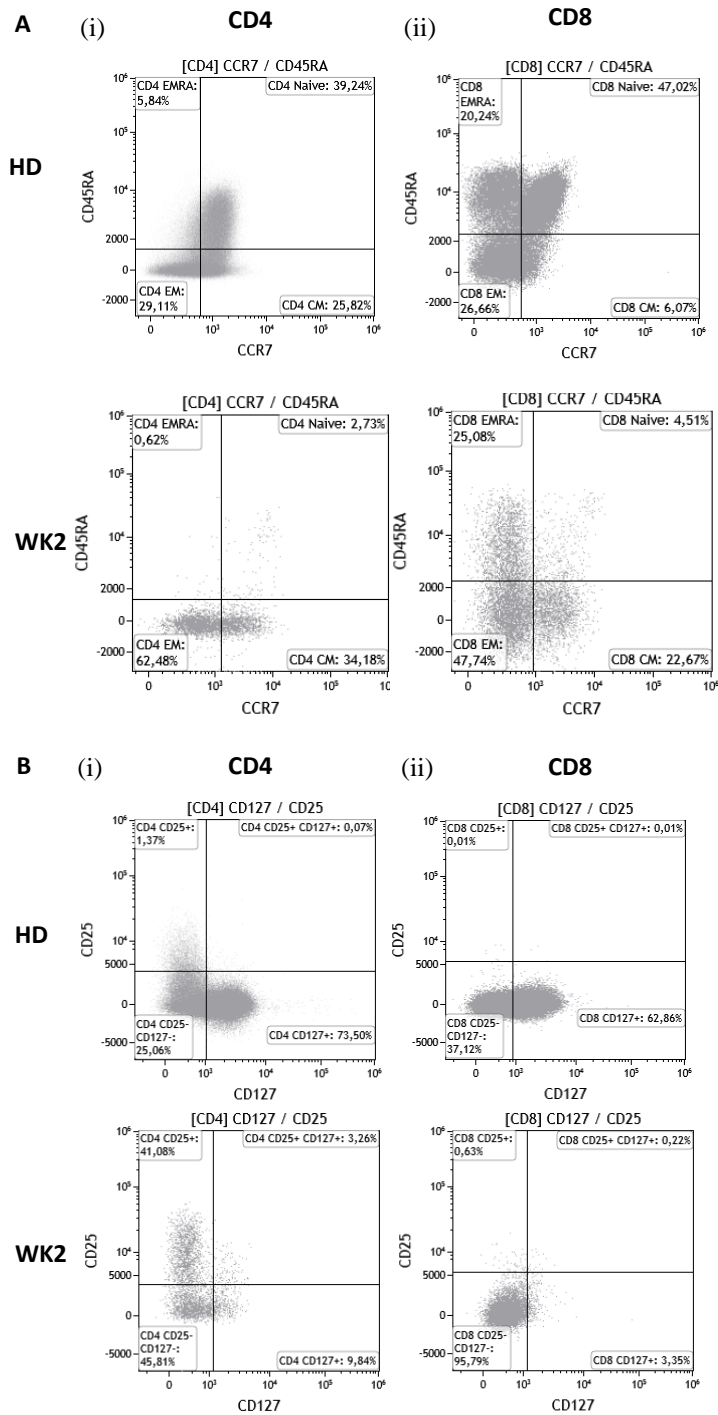
Figure S1. Autograft patients have a very different T cell phenotype at two weeks post-transplant compared to healthy donors, Related to Figure 2 Representative flow plots of CD45RA and CCR7 staining for CD4 T cells and CD8 T cells from a healthy donor and patient at WK2 post-autograft. **(B)** Representative flow plots showing CD25 and CD127 staining.
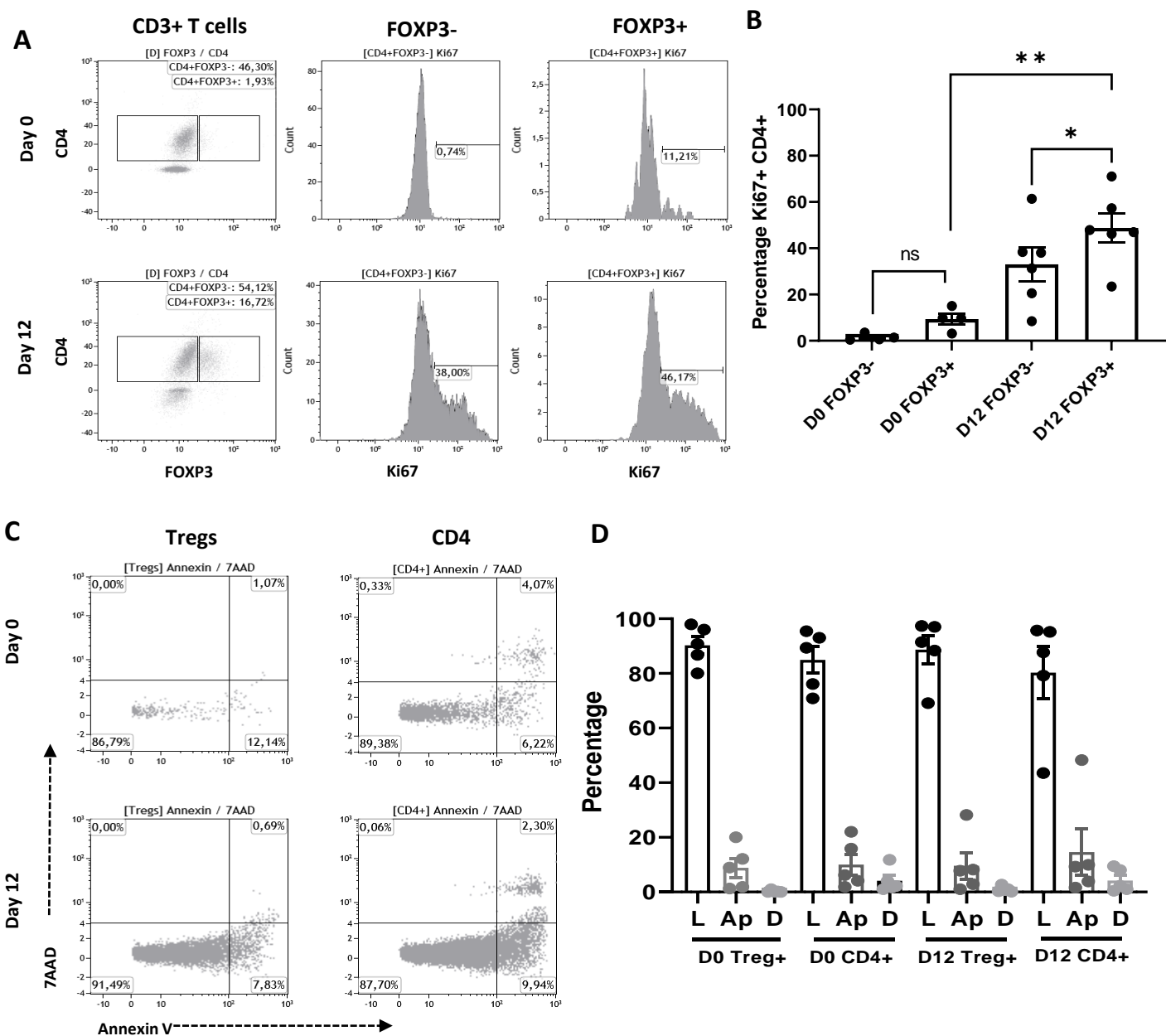
Figure S2. Increased proliferation of Tregs early after autologous stem cell transplant, Related to figure 5 (A) Representative FACS plot of paired D0 and D12 PBMCS showing FOXP3 staining on CD4 T cells and Ki67 staining on FOXP3- and FOXP3+ CD4 T cells. (B) Percentage of proliferating Ki67+ cells within the CD4+ FOXP3+ and CD4+FOXP3- T cells from blood samples collected at day 0 (D0, n=4) and day 12 (D12;. n=6) post-transplant. Statistical analysis was performed using Wilcoxon matched-pair signed rank test to compare FOXP3- and FOXP3+ for each time point. Mann-Whitney U test was performed to compare D0 and D12. (C) Representative FACS plots depicting Annexin V and 7AAD staining on paired D0 and D12 sample. (D)Percentage of Live(L; Annexin-7AAD-), Apoptotic (Ap; Annexin+7AAD-) and Dead (D; Annexin+7AAD+) cells within CD25+CD127- CD4+ T cells (Tregs) and whole CD4+ T cell population. No statistically significant differences were observed between the two time points. * represents p value <0.05, ** represents p value <0.01
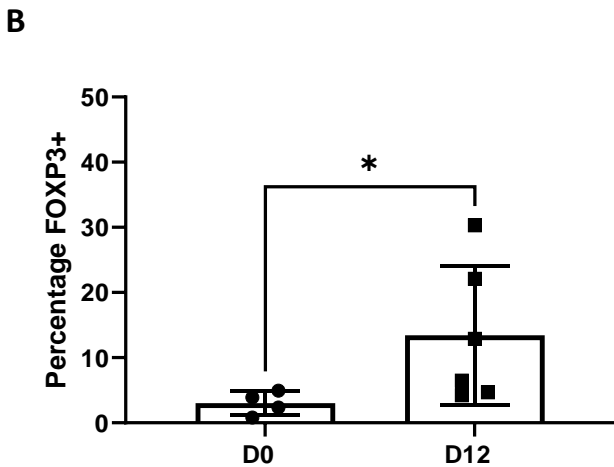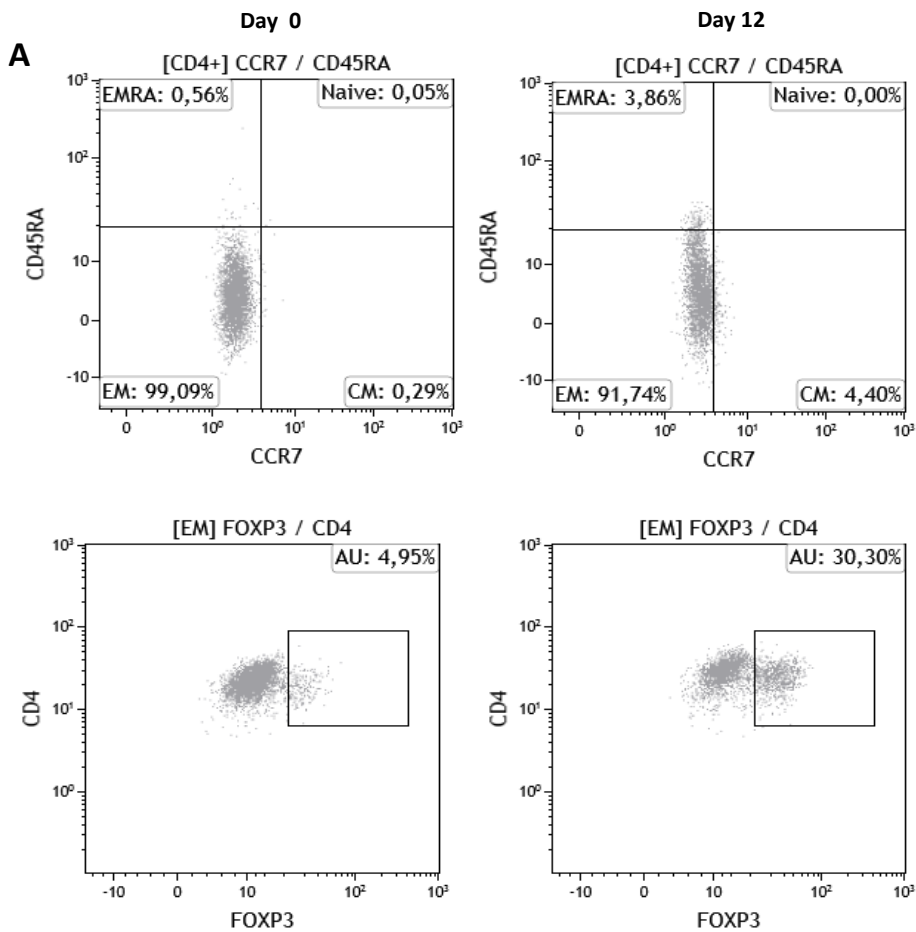
Figure S3. Proportion of FOXP3+ cells within EM CD4+ T cell population at D0 and D12 post-transplant, Related to figure 5 (A) Representative FACS plot of paired D0 and D12 PBMCS showing CD4 T cell subsets based on cell surface expression of CD45RA and CCR7 (upper panel) and FOXP3 staining (lower panel) on EM CD4+ T cells. (B) Percentage FOXP3+ cells within EM CD4+ T cells. Mann-Whitney U test was performed for statistical analysis. * represents p value <0.05
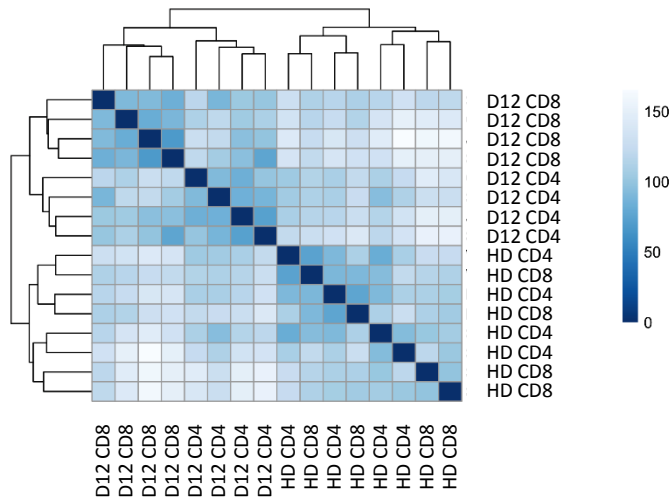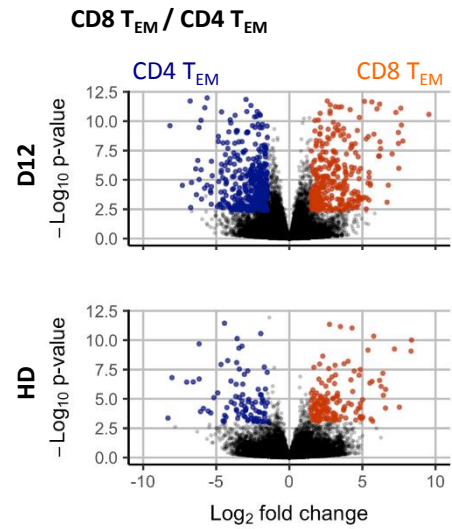
Figure S4. Sample distance matrix and Diversion of CD4 and CD8 T cell transcriptome at HD and at day 12 post autograft, Related to figure 5 (A) Sample distance matrix (Euclidean distance) of normalized gene expression data from RNA-seq of healthy donor (HD) and day 12 (D12) post autograft CD4 and CD8 effector T cells **(B)** Differential expression analysis results from CD8 vs CD4 effector T cell comparisons at day 12 or from healthy donors. Coloured points indicate differentially expressed genes in the comparison (Orange = UP in CD8 ; Blue=DOWN in CD8). Genes are deemed to differentially expressed if adjusted p-value <0.05 and absolute log2FC > 1.5.
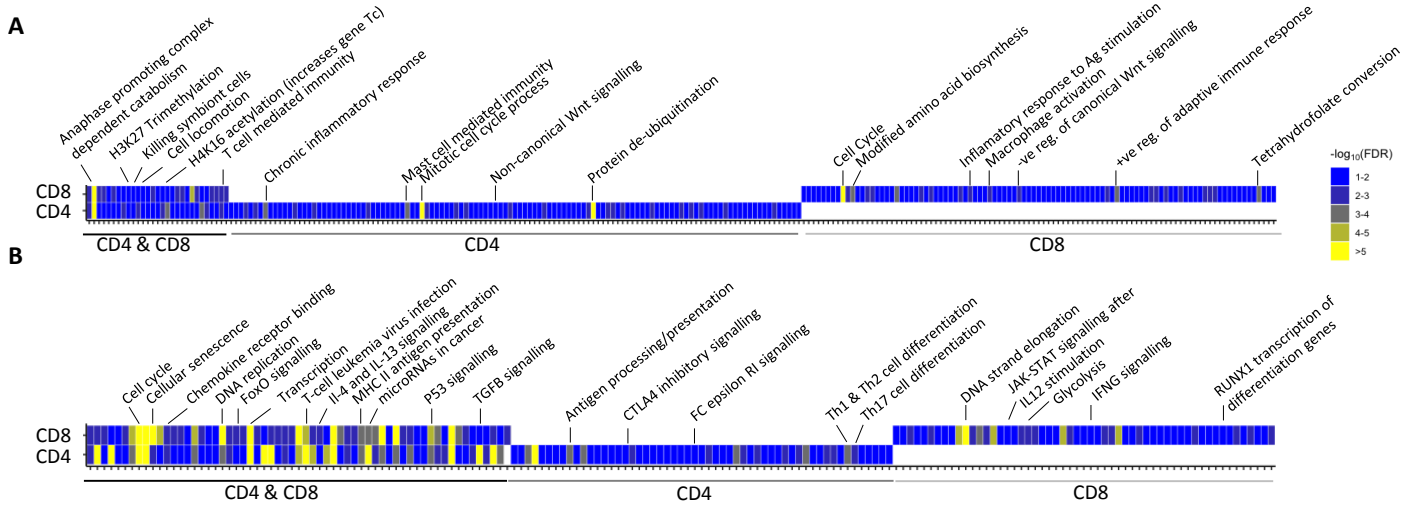
Figure S5. Functional enrichments within genes identified as being differentially expressed in effector memory T cells from patients at day 12 post-autograft vs healthy donors, Related to figure 6 Significant enrichments (FDR<0.1) of Biological Process **(A)** and Pathway **(B)** terms associated with genes differentially expressed in D12 CD4 or CD8 T cells compared to HD. Terms are ordered on the x axis from enrichments shared in both CD4 and CD8 DEGs to CD4 specific and CD8-specific DEGs
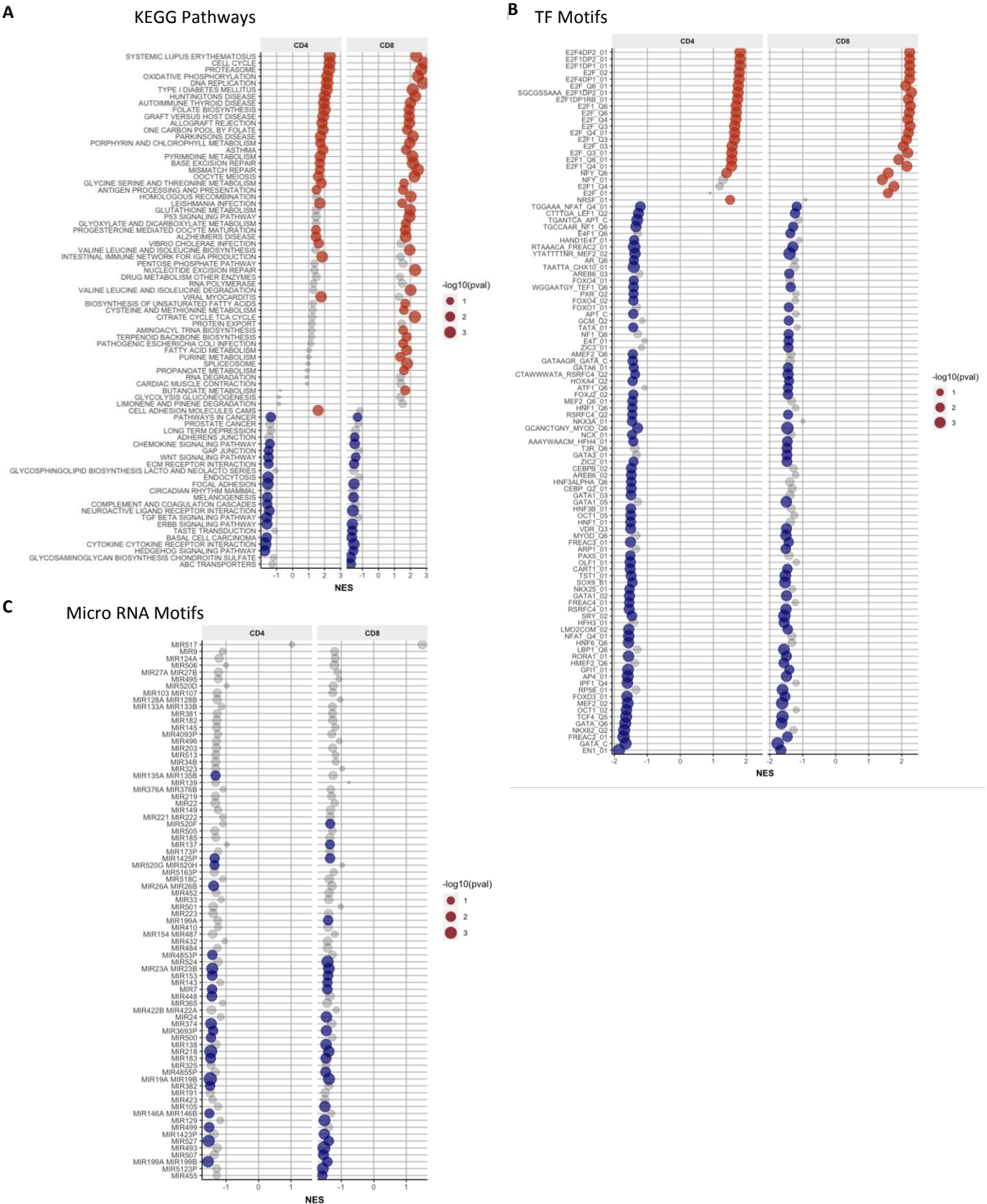
Figure S6. Gene Set Enrichment Analysis, Related to figure 7 (A) GSEA results of selected MSigDB KEGG pathway gene sets. GSEA of selected MSigDB Transcription factor binding motif gene sets **(B)** and selected MicroRNA binding motif sets **(C).** These motif sets comprise of genes containing at least one motif for the binding site of the transcription factor or MicroRNA. Shown are selected sets having FDR <0.2 in either CD4 or CD8 D12 vs HD comparisons. Colored circles indicate significant enrichments (FDR<0.1) towards genes upregulated (Red) or downregulated (blue) at D12 compared to HD.
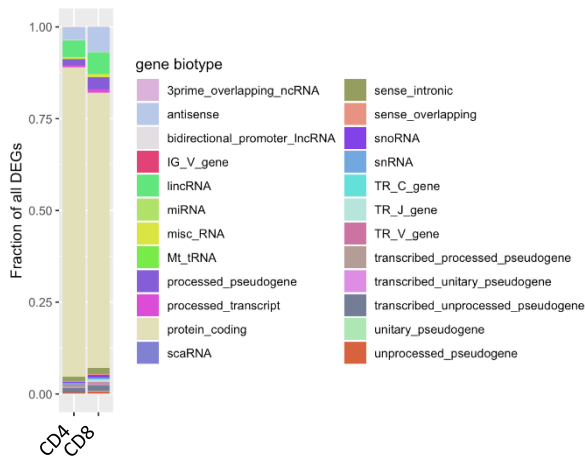
Figure S7. Proportions of gene biotypes in day 12 post autograft vs healthy donor differentially expressed genes, Related to figure 7. Proportions of annotated gene biotypes evident within genes identified as being differentially expressed in CD4 and CD8 effector T cells.
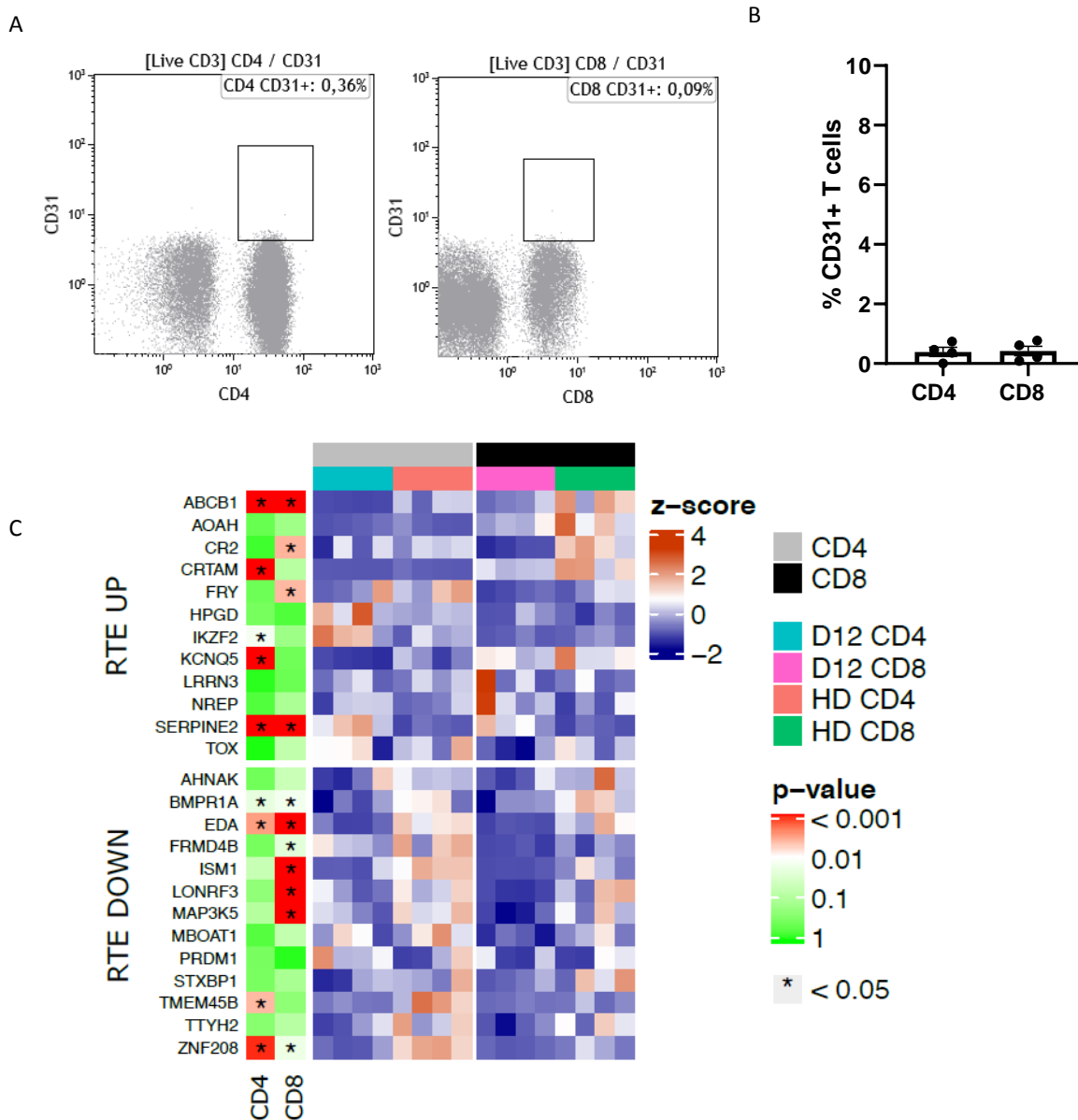
Figure S8. No phenotypic or transcriptional evidence to support presence of recent thymic emigrants is present at day 12 post-transplant, Related to figure 7 (A) Representative FACS plots depicting CD31 staining on CD4+ T cells and CD8+ T cells. (B) Percentage of CD31+ CD4 and CD8 T cells at day 12 post-transplant. (C) Expression profile of recent thymic emigrant (RTE) signature genes (Pekalski et al., 2017) in CD4/CD8 effector T cells from D12 post-autograft patients and healthy donors. p-values are from D12 vs HD differential expression analysis and are corrected for multiple testing.

Table S1. **Patient characteristics, Related to figure 1-7** (A) Characteristics of all patients included in the study (B) Characteristics of patients included in the transcriptomics analysis

Factor	Characteristic	A N (%)	B N(%)
Gender	Male	89 (64%)	2(50%)
	Female	51 (36%)	2(50%)
Median age (range)		62 (17-74)	60(53-70)
Diagnosis	Myeloma	98 (70%)	4(100%)
	Lymphoma	40 (28%)	0(0%)
	Other	2(1%)	0(0%)
Conditioning	Melphalan	101 (72%)	4(100%)
	LEAM	14 (10%)	0(0%)
	BEAM	22 (15%)	0(0%)
	Cyclo/TBI	1 (1%)	0(0%)
	BCNU/Thiotepa	3 (2%)	0(0%)
CMV status	Positive	69 (49%)	0(0%)
	Negative	70 (50%)	4(100%)
	Equivocal	1 (1%)	0(0%)

BEAM: carmustine (BiCNU), etoposide, cytarabine (Ara-C, cytosine arabinoside), melphalan; LEAM: lomustine, etoposide, cytarabine (Ara-C, cytosine arabinoside), melphalan; Cyclo/TBI: cyclophosphamide, total-body irradiation; CMV: cytomegalovirus

Transparent Methods

Sample cohort

Patients undergoing autologous stem cell transplant for myeloma or lymphoma at the Queen Elizabeth Hospital, Birmingham, UK were enrolled on the study following full written informed consent (15/WM/0194). All patient details are shown in Supplemental Table 1A. A control cohort of age-matched healthy donor samples was studied for comparison using leukocyte-enriched blood cones, residual from NHSBT donation.

Sample collection

Blood samples were collected post-conditioning but prior to stem cell infusion on day 0 (D0), and post-transplant on day 7 (D7) and on day 12 (D12). Blood was taken into sodium heparin tubes for flow cytometric analysis and serum tubes for assessment of cytokine concentrations. For all subsequent experiments, fresh blood-derived T cells were analysed. Serum was frozen and stored at –80°C for later use.

Phenotypic analysis of T cells

Peripheral blood mononuclear cells (PBMCs) were isolated by density gradient centrifugation. Mononuclear cells were surface stained with antibodies on ice for 20 minutes. T cell subsets were identified using the following monoclonal antibodies: αβTCR-Pacific blue (clone IP26, Biolegend, San Diego, US), CD4-APC/Cy7 (clone RPA-T4, BD Biosciences, New Jersey, US) and CD8 PerCPVio700 (clone BW135/80, Miltenyi Biotec, Bergisch Gladbach, Germany). Naive and memory populations were defined with CD45RA-AF700 (clone HI100, Biolegend) and CCR7-FITC (clone 150503, R&D Systems, Minneapolis, US) expression. CD25-PE/Cy7 (clone M-A251, BD Biosciences), CD127-BV510 (clone HIL-7R-M21, BD Biosciences), and CD95-AF647 (clone DX2, Biolegend) were included for phenotypic expression analysis. CD14-ECD (clone RMO52), CD19-ECD (clone

J3-119, Miltenyi Biotec) and CD56-PECF594 (clone B159, BD Biosciences) were added to gate out monocytes, B cells and NK cells. Propidium iodide (PI) was added immediately prior to acquisition to exclude dead cells. To identify Tregs, PBMCs were stained with fixable red LIVE/DEAD dye (Invitrogen, California, US) and above mentioned surface antibodies for 30 mins on ice. Cells were fixed by adding 1ml of 1X FOXP3 Fix/Perm solution (Biolegend) to each tube, vortexed and incubated at room temperature in the dark for 20 minutes, spun down and supernatant was discarded. Cells were then re-suspended in 1ml 1X BioLegend's FOXP3 Perm buffer, incubated at room temperature in the dark for 15 minutes, spun down and then re-suspended in 100 ul of 1X BioLegend's FOXP3 Perm buffer. anti-FOXP3-AF647 (clone 206D, Biolegend) was added and cells were incubated at room temperature in the dark for 30 minutes. Ki67 staining was performed at the same time along with anti-FOXP3 staining using anti-Ki67-PECy7 (clone Ki-67, Biolegend). Finally, cells were washed in PBS, spun at 2000rpm and re-suspended in 200ul of PBS. Data were acquired on Gallios followed by analysis using Kaluza software (both Beckman Coulter, Pasadena, US). The lymphocyte population was identified by forward scatter/side scatter dot plots and live T cells were identified by gating on PI–αβTCR+ cells. Clinical counts (lymphocytes per ml whole blood) were provided by the Queen Elizabeth Hospital for each patient. The absolute number of TCRαβ T cells was calculated using the clinical counts together with flow cytometric analysis of lymphoid subsets.

Quantification of serum analytes

ELISA assays (R&D systems) were performed to determine the concentration of IL-7, IL-15, IFN-γ and TGF-β in serum from patients at day 0 and day 12 or age-matched healthy donors. Plates were read using a iMark microplate reader (Bio-Rad Laboratories, California, US).

RNA sequencing, differential expression and functional enrichment analysis

RNA was isolated from FACS-sorted CD4+ and CD8+ effector (CD45RA-CCR7-) T cells isolated from healthy donor PBMCs (n=4) and day 12 post-autograft PBMCs (n=4). Patient characteristics are described in Table S1-B.

Total RNA isolation was performed following the manufacturer's instructions using the RNeasyPlus Micro Kit (Qiagen, Cat. No. 74134). In brief, the sorted cells were re-suspended in 350 µL Buffer BLT and vortexed. Equal amount of 70% Ethanol was added and the suspension was transferred to Rneasy spin column and spun for 15s at 10,000rpm. The flow through was discarded and the column was washed with Buffer RW1 and Buffer RPE. The final RNA was eluted in 30 µL RNase-free water. 10ng of RNA was used to prepare RNA libraries were prepared using a TruSeq Stranded Total RNA Library preparation kit and paired end sequencing performed on Illumina NextSeq. Reads were aligned to the human reference genome (hg19) with STAR aligner (Dobin, Davis et al. 2013) and raw read counts quantified with HTSeq (Anders, Pyl et al. 2015). Normalisation and differential expression analysis was performed using the DESeq2 package (Team 2013). Genes were considered differentially expressed if the adjusted p value (Benjamini Hochberg procedure (Benjamini and Hochberg 1995) was < 0.05 and absolute log2FC > 1.5. Gene Set Enrichment analysis was performed on published gene sets from MSigDB (Liberzon, Subramanian et al. 2011) using the R package FGSEA (Sergushichev 2016). Pathway analysis was performed on lists of differentially expressed genes using gProfiler (Raudvere, Kolberg et al. 2019) Visualisations were generated using the R package ggplot2 (Wickham 2016).